arXiv:cond-mat/9610171v1 23 Oct 1996

# Temperature and magnetic field dependence of the lattice constant in spin–Peierls cuprate $CuGeO_3$ studied by capacitance dilatometry in fields up to 16 Tesla

T. Lorenz, U. Ammerahl, T. Auweiler, and B. Büchner
*II. Physikalisches Institut, Universität zu Köln, Zülpicher Str. 77, 50937 Köln, Germany*

A.Revcolevschi and G. Dhalenne
*Laboratoire de Chimie des Solides, Université Paris-Sud, 91405 Orsay Cédex, France*
(February 1, 2008)

## Abstract

We present high resolution measurements of the thermal expansion coefficient and the magnetostriction along the $a$–axis of $CuGeO_3$ in magnetic fields up to 16 Tesla. From the pronounced anomalies of the lattice constant $a$ occurring for both temperature and field induced phase transitions clear structural differences between the uniform, dimerized, and incommensurate phases are established. A precise field temperature phase diagram is derived and compared in detail with existing theories. Although there is a fair agreement with the calculations within the Cross Fisher theory, some significant and systematic deviations are present. In addition, our data yield a high resolution measurement of the field and temperature dependence of the spontaneous strain scaling with the spin–Peierls order parameter. Both the zero temperature values as well as the critical behavior of the order parameter are nearly field independent in the dimerized phase. A spontaneous strain is also found in the incommensurate high field phase, which is significantly smaller and shows a different critical behavior than that in the low field phase. The analysis of the temperature dependence of the spontaneous strain yields a pronounced field dependence within the dimerized phase, whereas the temperature dependence of the incommensurate lattice modulation compares well with that of the dimerization in zero magnetic field.

PACS: 64.70.Kb,65.70.+y,75.40Cx,75.80+q

Typeset using REVTEX

## I. INTRODUCTION

Since the discovery of a spin–Peierls transition in the inorganic cuprate $CuGeO_3$ by Hase et al. [1] this unusual magnetoelastic transition occurring in quasi one–dimensional antiferromagnetic insulators has again attracted considerable attention. Compared to the well known organic spin–Peierls systems [2] the structure of $CuGeO_3$ is rather simple. This fact and the possibility of growing large high quality single crystals allows for a much better study of the spin–Peierls phenomena in $CuGeO_3$ than in the organic compounds.

Most properties expected from the well developed theory of the spin–Peierls transition, e.g. the Cross Fisher (CF) theory [3,4], are observed in $CuGeO_3$. For example elastic neutron and x–ray scattering show a doubling of the orthorhombic unit cell below the transition temperature $T_{SP} \simeq 14.3$K leading to two non–equivalent Cu sites in the magnetic chains. This lattice distortion leads to alternating Cu–O–Cu superexchange paths, i.e. alternating intrachain magnetic exchange constants. Also in agreement with the CF theory a gap in the magnetic excitations is observed [5], which scales with the structural order parameter, i.e the dimerization. Whereas these properties of the dimerized (D) phase of $CuGeO_3$ seem to be well represented by a model of spin–1/2 Heisenberg chains with a spin–Peierls transition, some significant deviations from this most simple treatment are present in the uniform (U) phase, i.e. for $T > T_{SP}$. Most strikingly the magnetic susceptibility in the U phase of $CuGeO_3$ disagrees with the temperature dependence calculated for one–dimensional spin–1/2 Heisenberg chains [1,6,7]. There is evidence that the corrections which are necessary to explain the magnetism in the U phase also influence the spin–Peierls transition. It is argued for example that due to a frustration of the magnetic exchange in the quasi one–dimensional chains [6,8] $T_{SP}$ is strongly enhanced in $CuGeO_3$.

The influence of a magnetic field represents a further characteristic feature of the spin–Peierls transition, which can be directly compared to the different theoretical predictions. Due to the additional Zeeman term in the Hamiltonian the nonmagnetic dimerized phase is destabilized when applying a magnetic field. Consequently an additional phase with a finite susceptibility occurs at high magnetic fields, in $CuGeO_3$ for $H \gtrsim 12$ Tesla. An incommensurate lattice modulation has been predicted theoretically for this I phase and was recently observed by x–ray diffraction [9]. However, the knowledge about this phase is still very limited, e.g. the spatial character of the incommensurate lattice modulation – domain walls or sinusoidal modulation – is still a subject of debate.

The theoretical H–T phase diagrams which have been calculated with different treatments of spin 1/2 Heisenberg (or XY) chains differ significantly. A detailed experimental determination of the phase diagram in $CuGeO_3$ therefore allows for a test of these theories and future descriptions incorporating e.g. a frustration of the magnetic exchange. The theories yield different predictions for the positions of the three phase boundaries – U/D, U/I, and D/I – in reduced field and temperature scales. Moreover, the CF theory and the earlier theory by Bulaevskii et al. [10] predict a discontinuous first order D/I transition, whereas a continuous transition is obtained within the soliton picture [11].

So far the H–T phase diagram of $CuGeO_3$ has been mainly studied via measurements of the magnetization. The phase boundaries roughly agree with the predictions of the CF theory [12], though when analyzing the data in detail some deviations seem to be present. Up to now there is only little information on the thermodynamic and structural properties

in high magnetic fields, particularly with regard to the incommensurate phase.

In this paper we will present a detailed study of the coefficient of the thermal expansion $\alpha$ along the $a$–axis in magnetic fields up to 16 Tesla [13]. As shown in Ref. [14] there is a very large anomaly of $\alpha$ at the U/D transition. Therefore, a very detailed investigation of the H–T phase diagram is possible via measurements of $\alpha$ in external fields. Moreover, $\alpha$ represents a thermodynamic property similar to the specific heat. Therefore it allows to study the nature of the different transitions and the critical behavior. Furthermore, $\alpha$ is per definition a structural property, i.e. the temperature dependence of the relative lattice constant. Because of that the giant anomalies of $\alpha$ at $T_{SP}$ measure the development of spontaneous strains ($\epsilon$) at the U/D transition. The spontaneous strains of the D phase in $CuGeO_3$ are surprisingly rather large ($\simeq 10^{-5}$) and have been observed not only by high resolution capacitance methods but also by diffraction techniques [15–17].

A comparison with neutron diffraction data reveals that the spontaneous strains are proportional to the squared order parameter of the spin–Peierls transition. Thus, the high resolution measurements of $\alpha$ yield a precise measurement of the order parameter in the D–phase as a function of both temperature and magnetic field. In addition, we will show that reduced but still large spontaneous strains are present in the I phase, and thus the temperature dependence of the incommensurate lattice modulation can also be determined from our data.

The thermal expansion measurements performed at fixed fields yield information on the phase transitions occurring as a function of temperature. In order to allow for the discussion of a complete H–T phase diagram, we will also present some measurements of the magnetostriction [18], i.e. the changes of the lattice constant as a function of a magnetic field at a fixed temperature. The magnetostriction shows anomalies at field driven phase transitions and thus it is possible to determine the D/I phase boundary which is nearly parallel to the temperature axis in the H–T phase diagram and therefore difficult to analyze by thermal expansion measurements.

The paper is organized as follows. After a short description of the capacitance dilatometer we will give an overview of the experimental observations in Section III. The pronounced differences between the lattice constants of the three phases of $CuGeO_3$ are already visible in these raw data. The H–T phase diagram obtained from our measurements is presented and discussed in section IV. The following section V "*Field dependence of the thermal expansion and the spin–Peierls order parameter*" is divided into five parts. Before discussing the influence of the magnetic field on the lattice constant in detail we will shortly repeat some results extractable from $\alpha$ in zero magnetic field. Then we are going to discuss the reduction of the anomaly of $\alpha$ at $T_{SP}$ with increasing field by considering its relationship to the anomaly of the specific heat. The next part deals with the critical behavior of the order parameter, which differs for the U/D and U/I transitions, respectively. Hereafter the magnetic field dependence of the dimerization at low temperatures, which is found to be extremely weak in the D phase, and the pronounced discontinuous changes of the spontaneous strains at the field driven D/I transition are discussed. Finally in the last part of section V the temperature dependencies of the order parameter well below $T_{SP}$ are analyzed. We find a remarkably strong field dependence within the D phase, whereas the temperature dependence of the incommensurate modulation compares well with that of the dimerization in zero magnetic field.

## II. EXPERIMENTAL

The single crystal of $CuGeO_3$ used for the present study was cut from a large crystal (80 mm along the $a$–axis) grown by a floating zone technique [19]. The sample is of cylindrical shape with dimensions of about 6x5x8.3 $mm^3$ for the $a$–,$b$–, and $c$–axis, respectively. Various experimental investigations on samples prepared in this way have already been published. Some details of structural and magnetic properties of these crystals are described e.g. in Ref. [20].

The measurements were carried out with a new capacitance dilatometer. It was originally designed to allow for measurements of the coefficient of the thermal expansion $\alpha \equiv \frac{1}{L} \cdot \frac{\partial L}{\partial T}$ ($L$: length of the sample) in fixed external fields only. Besides, it enables to measure the magnetostriction, i.e. the field induced length changes $\frac{\Delta L(H)}{L}$ at fixed temperatures. Both types of measurement can be performed during a single run, i.e. for exactly the same orientation of the crystal in the dilatometer. During the measurements the dilatometer is mounted into an evacuated stainless steal tube, which fits into the 40 mm bore of a superconducting 16 Tesla magnet. Although the new dilatometer is based on our conventional one described in Ref. [21] some significant differences exist. The main difference is a thermal decoupling between the sample and the plate capacitor, i.e. the temperature of the sample is changed, but the capacitor is thermally coupled to the liquid He bath. Therefore no thermal expansion of the capacitor itself occurs during a measurement and the capacitance changes mainly reflect the length changes of the sample ("small cell effect"). Moreover, the mass whose temperature has to be controlled is drastically reduced. It only consists of the sample itself and a small sample holder ($\simeq$ 50 g Cu). This allows for a rapid and accurate control of the temperature using e.g. a software PID-technique. The temperature range is restricted by the maximum heater current to $T \lesssim 200K$.

We use platinum (Pt 103) and "Cernox CX–1050" temperature sensors (Lake Shore) for temperatures above and below 100K, respectively. The field dependence of the latter can be neglected, since its magnetoresistance is extremely small – the deviation is 2% at 2.5K for H = 16 Tesla and rapidly decreases with increasing T. The length changes of the sample are calculated from the capacitance changes measured by a temperature stabilized capacitance bridge (Andeen–Hagerling) with a resolution of $5 \cdot 10^{-7}$ pF. Thus, length changes of less than 0.01 Å can principally be resolved. Due to mechanical vibrations etc. the resolution is limited to $\simeq 0.1$ Å in practice. The thermal expansion measurements are performed in a continuous mode, i.e. capacitance data are recorded while the temperature is continuously increased with a small and constant rate, usually $2-3$ mK/s. For calibrating the dilatometer we measured the well known [22] thermal expansion of aluminum samples of several lengths (4 to 8 mm). The calibration was checked by measuring a 5mm copper sample. The relative resolution, i.e. the scatter of the data, amounts to $\simeq 5 \cdot 10^{-8}$/K and the deviation to the data reported in the literature [22] is less than $\simeq 1 \cdot 10^{-6}$/K for temperatures up to 200K. In the temperature range below 45K, which is considered in this paper only, the maximum deviation is even less than $\simeq 1 \cdot 10^{-7}$/K.

For the magnetostriction measurements temperature is held constant and length changes are detected while the magnetic field is swept from 0 up to 14 (or 16) and back to 0 Tesla with a rate of $2.5 - 4$mT/s. For calibration we performed magnetostriction measurements on a 5mm silicon sample. The cell effect – due to magnetic impurities and eddy currents

which cause stresses on the dilatometer via the Lorentz force – amounts up to 250Å, which corresponds to $\simeq 5 \cdot 10^{-6}$ for a 5mm sample. The reproducibility of this cell effect and thus the accuracy of the absolute values of the magnetostriction $\Delta L/L$ is better than $\simeq 5 \cdot 10^{-7}$. The scatter in $\Delta L/L$ amounts to $\simeq 2 \cdot 10^{-9}$, which corresponds to 0.1Å as mentioned above.

## III. RESULTS

### A. Thermal Expansion

Since some organic spin-Peierls compounds show a pronounced hysteresis of the magnetic susceptibility [23,24] as well as of the structure [25] when changing the magnetic field at low temperatures, all measurements of $\alpha$ were performed in the field cooled mode. After applying the magnetic field well above $T_{SP}$, usually at $T \simeq 25$K, the sample was cooled down to 4K (or 2K). Then the data were taken while the temperature was continuously increased with a rate of 2 mK/s. In order to check the presence of hysteretic behavior we have also performed some measurements in the zero field cooled mode, e.g. after applying magnetic fields of H = 11T and H = 14T at 4K and after decreasing the magnetic field from 14T to 11T at 4K. In all cases studied the data agree with those obtained from the field cooled measurements at the same magnetic fields. In $CuGeO_3$ the hysteresis of the lattice constants as well as that of other properties [26–28,12] in the H–T phase diagram is apparently rather weak and restricted to a very narrow field range, i.e. the data in Figs. 1 and 2 represent the behavior of the lattice constant $a$ in thermal equilibrium except for the region $H \simeq 12.5$T (see below).

As shown in an earlier publication [14] there is a very pronounced decrease of $\alpha$ along the $a$–axis at the spin–Peierls transition in zero magnetic field. This decrease is related to a large negative uniaxial pressure dependence $dT_{SP}/dp_a \simeq -4$K/GPa on the one hand and to a spontaneous lengthening of the $a$–axis in the dimerized phase on the other hand. Fig. 1 gives an overview of the changes of the thermal expansion coefficient along the $a$–axis occurring as a function of magnetic field. A pronounced field dependence of $\alpha$ is present only below 20K, i.e. in the spin–Peierls phase. First of all the transition temperature $T_{SP}$ reduces with increasing field, a result known e.g. from measurements of the susceptibility [28,29]. In addition, a change of the anomaly of $\alpha$ as a function of the magnetic field is apparent from Fig. 1. In all cases the phase transition shows up by a pronounced decrease of $\alpha$. However, note that in Fig. 1 the anomaly for H = 14T is distinctively smaller than that for H = 8T, whereas the sizes of the anomalies for H = 8T and H = 0T are very similar.

This nonlinear change of the size of the anomalies is related to the different low temperature phases occurring as a function of magnetic field. In H = 8T the anomaly still arises from the spin–Peierls transition between the U and D phases [26,28,9], whereas the anomaly of $\alpha$ for H = 14T is due to a phase transition between the U the I phases. Although the anomaly for H = 14T is reduced in size, a clear structural change between the U and I phases of $CuGeO_3$ is inferred from these data. Moreover, this transition is strongly pressure dependent and leads to a spontaneous lengthening of the $a$–axis, similar to that in zero magnetic field.

Fig. 2 shows an expanded view of the temperature and magnetic field dependence of $\alpha$ up to 17.5K and for $0T \leq H \leq 16T$. With increasing magnetic field the anomaly of $\alpha$ is systematically shifted to lower temperatures, reflecting the decrease of the transition temperature

with increasing magnetic field. This decrease amounts to about $T_{SP}(0) - T_{SP}(H) \simeq 2K$ for fields up to H = 11T and to $\simeq$ 4K for H = 16T, respectively. Considering the shape and size of the anomalies the curves can be clearly classified into three groups: (i) Up to 12 Tesla the anomalies remain nearly unchanged. (ii) A very pronounced decrease of "$\Delta\alpha$" as a function of the magnetic field is present in the rather small field range between 12T and 13T. Besides the strong field dependence this second group of curves is characterized by additional anomalies occurring below 10K. As shown in Fig.3 very strange thermal expansions indicating the presence of several phase transitions as a function of temperature are found in the entire field range between 12T and 13T, most pronounced for H = 12.5T (see Fig. 3). (iii) In the field range between 13T and the maximum field of 16T again only one transition is present. The sizes of the anomalies are much smaller than those at low fields and they further reduce with increasing magnetic field. Despite of the limited field range for the investigation of this third group a stronger magnetic field dependence of the anomaly size than in the first group (H < 12T) is apparent even from the raw data.

The different groups of curves reflect the different kinds of phase transitions. Below 12 Tesla there is a transition between the U and D and above 13 Tesla between the U and I phases. In the field region 12T $\leq$ H $\leq$ 13T the three phase boundaries U/D, U/I, and D/I meet in a tricritical point. At temperatures below this tricritical point two transitions are expected with increasing magnetic field (D/I and I/U). A sequence of transitions is also possible and present (see Fig. 3) as a function of temperature pending on the details of the D/I phase boundary, which is nearly horizontal in the H–T phase diagram, i.e. occurring at a nearly constant magnetic field.

From the data presented so far it becomes apparent that all transitions between the three phases of $CuGeO_3$ lead to pronounced anomalies of the thermal expansion coefficient, i.e. each phase transition causes spontaneous strains. It should be mentioned that a dimerization alone, which is characterized by the development of alternating distances between nearest neighbors, i.e. an antiferro distortion, does not necessarily lead to spontaneous strains. Especially, within the CF theory pressure dependencies of $T_{SP}$ and thus anomalies of the thermal expansion coefficients are obtained only, if one adds an anharmonic coupling between elastic degrees of freedom and zone boundary phonons [30,31]. Such a coupling is of course no general property of the spin–Peierls transition and thus the pressure dependencies strongly differ for the spin–Peierls compounds [30,31].

### B. Magnetostriction

Whereas the measurements of thermal expansion are a very sensitive probe of the U/D and U/I phase transitions, it is rather difficult to determine the D/I phase boundary since the temperature dependence of the latter is very small. Therefore we also performed measurements of the magnetostriction, i.e. measurements of the magnetic field induced changes of the lattice constant $a$ at a fixed temperature, where the D/I-phase boundary is crossed almost perpendicular.

In Fig. 4 we show $\Delta a(H)/a(H = 0)$ obtained with increasing magnetic field at several temperatures between 3 and 18K. At the lowest temperature there is only an extremely small magnetostriction in the D phase and at $H_{D/I} \simeq 12.5$ Tesla a large jumplike decrease of the lattice constant $a$ occurs reflecting the first order phase transition between the D and

the I phase. With increasing temperature the "jump" of the lattice constant at the D/I transition strongly decreases indicating that the phase transition gradually changes from a discontinuous to a continuous one. Note, however, that $H_{D/I}$ and the total magnetostriction up to 14 Tesla, i.e. $a(14T)-a(0T)$, remain roughly constant below 11K. Moreover, a large magnetostriction is found in the D phase in this temperature range. A comparison with the thermal expansion data in Fig. 2 shows that all magnetostriction curves obtained in this temperature range reflect differences of the lattice constant between the D and the I phases. The gradual change from a clearly first order transition to a continuous one can also be extracted from the hysteresis of the magnetostriction around $H_{D/I}$ (see inset of Fig. 4). At low temperatures a small hysteresis with a maximum value of about 0.2 Tesla (at $T\simeq 3K$) is determined when comparing the measurements with increasing and decreasing magnetic field. With increasing temperature the amount of this irreversibility systematically decreases and vanishes for $T\gtrsim 11K$.

At temperatures between $\simeq$ 11K and 14.5K, i.e. for $T_{SP}(0T) > T > T_{SP}(12T)$ (see Fig. 2) the field driven transitions are no longer between the D and I phases. The still very pronounced and continuous decrease of the lattice constant $a$ up to a critical field now reflects the continuous phase transition between the low field D and the high temperature U phase of $CuGeO_3$. In contrast to the behavior at lower temperatures both the transition field and the total magnetostriction rapidly decrease with increasing temperature. The first observation arises from the decrease of $T_{SP}$ as a function of the magnetic field (see Fig. 2), which implies a decrease of $H_{D/U}$ with increasing temperature. The second observation reflects the temperature dependence of the spontaneous strain, i.e. the continuous increase of the structural difference between the D and U phases with decreasing temperature.

At temperatures above 14.5K no phase transition is found. However, a finite magnetostriction is clearly observable also in the U phase. Note that in contrast to the findings at lower temperatures the lattice constant $a$ now *increases* with increasing magnetic field. This magnetostriction in the U phase is not related to fluctuations of the spin–Peierls order parameter. It measures the magnetoelastic coupling in $CuGeO_3$, which is a precondition for the occurrence of a spin–Peierls transition [8]. It should be mentioned that this positive magnetostriction is found in the entire temperature range studied, i.e. up to 80K. A detailed discussion of the magnetoelastic coupling in the uniform phase as extracted from the magnetostriction and its anisotropy will be given in a forthcoming publication. The finite and slightly temperature dependent magnetostriction in the U phase implies a field dependence of the thermal expansion for $T > T_{SP}$. However, in agreement with the findings presented in Fig. 1 this field dependence is estimated to be extremely weak. As an upper limit for the difference $\alpha(0T) - \alpha(14T)$ we obtain $2 \cdot 10^{-8}/K$ for $20K < T < 80K$ corresponding to a relative change of $\alpha$ smaller than one percent. However, this finite magnetostriction in the U phase has to be taken into account for a quantitative comparison of the results of thermal expansion and magnetostriction measurements at low temperatures (see below).

## IV. H–T PHASE DIAGRAM

From the measurements of magnetostriction and thermal expansion it is possible to determine a complete and precise H–T phase diagram of $CuGeO_3$ since both quantities show pronounced anomalies at the different phase transitions. The anomalies of the magnetostric-

tion give the fields at the D/I and D/U phase transitions at different temperatures while those of $\alpha$ give the temperatures at the U/D and U/I transitions at different magnetic fields. It is apparent from the raw data presented so far that (i) the phase boundaries in $CuGeO_3$ follow the characteristic course expected for the spin-Peierls transition and that (ii) our observations are in rough agreement with the findings from other properties, e.g. the magnetization [12,28]. We did, however, not observe any anomaly of the thermal expansion or magnetostriction at H = 8 Tesla, where Poirier et al. found evidence for an additional phase boundary from ultrasonic studies [26].

The $\lambda$–like shape of the anomalies of $\alpha$ but also of the specific heat [32] signal the presence of pronounced fluctuations in $CuGeO_3$, which have to be taken into account when determining the transition temperatures. In literature quite different ways have been used to define $T_{SP}$ from the anomaly of the specific heat [33,32]. Ignoring the fluctuations and describing the anomaly as a broadened mean field step as in Ref. [33] one would obtain a transition temperature of $\simeq$ 14.5K for our crystal. However, this description is apparently not appropriate for our more homogeneous sample. If one assumes a (nearly) symmetric shape of the anomaly on a reduced temperature scale and a linear regular part [32], i.e. the behavior expected for critical fluctuations, the transition temperature is distinctively smaller. It is found close to the maximum of $C_p$ or the minimum of $\alpha$, i.e. at 14.16K for our crystal. However, the experimentally observed anomalies of the thermodynamic properties of $CuGeO_3$ all show a pronounced asymmetry even close to "$T_{SP}$". Therefore the temperature at the minimum of $\alpha$ only yields a lower limit for the transition temperature. In this paper we have defined $T_{SP}$ at the maximum slope of the anomaly yielding $T_{SP}$ = 14.35, which lies in between the two extreme values mentioned above. We emphasize that, despite of this rather large uncertainty of the absolute value, the decrease of $T_{SP}$ as a function of H is obtainable with very high precision (better than $\pm$0.05K) from our data, e.g. from the shift of the minimum in $\alpha$, since the shape of the anomalies does not change significantly (see below).

In Fig. 5 the H–T phase diagram of $CuGeO_3$ for fields parallel to the $a$–axis is displayed. The transition fields measured via the magnetostriction are defined in a similar way as $T_{SP}$, i.e. at the maximum value of the field derivative. As visible in Fig. 5 the boundaries obtained from the two experimental methods perfectly agree. For the transition fields between the D and I phases two values are given representing the hysteresis at this phase transition. The lower (higher) value corresponds to the transition field found with decreasing (increasing) magnetic field. The inset of Fig. 5 shows the D/I phase boundary on a smaller field scale. The hysteresis can be clearly resolved at least up to about 10K. This hysteresis and the shape of the anomalies of the magnetostriction (see Fig. 4) show that the field driven D/I transitions are of first order. The shapes of the additional anomalies in the thermal expansion (Fig. 3), which show up very close to this phase boundary, also indicate a weakly first order D/I transition as a function of temperature.

Similar to the experimental results found in the organic spin–Peierls compounds [34] the H–T phase diagram of $CuGeO_3$ does not support the soliton theories of the spin–Peierls transition. Most of the arguments given in Ref. [34], which favor the traditional theories, e.g. the CF theory, in the case of TTF–BDT(Au) also hold for $CuGeO_3$. For example the soliton theory predicts a continuous D/I transition, whereas experimentally a first order transition is found. Moreover, the D/I transition is predicted to occur at $g\mu_B H_{D/I} \simeq 0.6E_0$,

where $E_0$ denotes the spin excitation gap at zero temperature [35,36]. Using the excitation gap derived from inelastic neutron scattering studies [37], the D/I transition should occur at $H_{D/I} \simeq 8.5$T, which is significantly smaller than the experimental value.

The experimental data agree much better with the calculations of Cross [4] and the earlier treatment of Bulaevskii et al. [10]. A simple comparison to these calculations is possible by considering firstly the decrease of $T_{SP}$ at small magnetic fields and secondly the tricritical point, where the U/D, U/I, and I/D phase boundaries meet. Both theories yield in leading order a quadratic decrease of $T_{SP}(H)$ with H, i.e. $(T_{SP}(H)-T_{SP}(0))/T_{SP}(0) = -\tau\cdot\left(\frac{g\,H}{2\,T_{SP}(0)}\right)^2$. The predicted quadratic field dependence is confirmed by our data up to about 6T. The prefactor amounts to $\tau = 0.21$K/T, which agrees with the data reported by Poirier et al. [26]. Taking into account the g–factor of 2.15 for fields parallel to the $a$–axis [38] the theoretical treatments of Bulaevskii et al. and Cross yield $\tau = 0.19$K/T and $\tau = 0.16$K/T, respectively. The tricritical point is derived from our measurements at $H_c = 12.25$ Tesla and $T_c = 11$K (see Fig. 5). The reduced values $\frac{T_c}{T_{SP}(0)} = 0.77$ and $\frac{g\,H_c}{2\,T_{SP(0)}} = 0.92$T/K can directly be compared to theory. Bulaevskii et al. find ratios of 0.63 and 1.08 [10], whereas Cross calculates 0.77 and 1.03 [4] for the reduced tricritical temperature and field, respectively. Apparently, our data very well agree with the prediction of Cross, especially with regard to $T_c$. The deviations from the calculations of Bulaevskii are somewhat larger. This is expected for quite general reasons, since more reliable results are obtained from Cross' Luther Peschel treatment of the one–dimensional spin excitations than from the Hartree Fock approach used by Bulaevskii et al..

In Fig. 5 the phase boundaries calculated by Cross are compared to our experimental findings. As mentioned above there are clear discrepancies. However, the shape of the boundaries is very similar and there is an easy way to obtain a perfect agreement between the theoretical curve and the experimental U/D phase boundary. As also shown in Fig.5 the experimental data follow a theoretical curve, when the reduced field scale is divided by 1.12 (dotted line). The "effective" magnetic field, which acts in $CuGeO_3$, seems to be larger than that calculated. Cross himself already gives some possible reasons for this kind of deviation [4]. For example, using a too small zero–temperature susceptibility to derive the phase diagram causes an "effective" magnetic field that is also too small. Thus, the discrepancy between theoretical and experimental H–T phase diagrams might be related to the striking discrepancy between the measured and calculated susceptibility of $CuGeO_3$ in the U phase. The latter has been attributed to a next nearest neighbor exchange [6,7] in the quasi–one dimensional chains in $CuGeO_3$. Recently, first calculations of the H–T phase diagram within a model incorporating a next nearest neighbor exchange have been published [39]. At the present stage these calculation do, however, not improve the agreement with the experimental data.

Since particular properties of $CuGeO_3$ might influence the H–T phase diagram, a comparison to the findings in other spin–Peierls compounds seems worthwhile [40]. As shown by Hase et al. [12,41] the H–T phase diagrams of all spin–Peierls compounds roughly coincide on reduced temperature and field scales. However, some small but systematic differences are present. This is most clearly visible for the D/I phase boundary, which is located at larger (reduced) magnetic fields in the organic compounds than in $CuGeO_3$. Despite of the rather large scatter of the data for the organic compounds the same trend is also found when comparing the D/U boundaries of the organic compounds to our data of $CuGeO_3$. Thus,

an enhanced "effective" magnetic field, which destabilizes the D phase of $CuGeO_3$, can also be inferred from a comparison to the organic spin–Peierls compounds.

In order to compare the phase boundaries to the I phase one has to take into account a particular property of the organic spin–Peierls compounds. A pre–existing soft phonon, which stabilizes the commensurate lattice deformation [10,4], seems to be a characteristic feature of all these systems. In $CuGeO_3$ the experimentally observed field at the D/I transition is rather low compared to the calculated one. Moreover, the transition temperatures at the U/I transitions are larger and less field dependent than predicted by theory. Thus, the H–T phase diagram yields no evidence that details of the phonon spectrum favor the D phase compared to the other phases. In agreement with this conclusion drawn from the H–T phase diagram no pre–existing soft phonon has been observed so far in $CuGeO_3$.

## V. FIELD DEPENDENCE OF THE THERMAL EXPANSION AND THE SPIN–PEIERLS ORDER PARAMETER

The presented data of the magnetostriction and the thermal expansion in magnetic fields do not only allow for an accurate determination of the phase diagram. Information on thermodynamic properties of the phase transition as well as information about the field and temperature dependence of the structure are also obtained from these high resolution measurements of the lattice constant $a$. Before we are going to discuss the field dependencies in detail we shortly remind on the basic conclusions drawn from the zero field data in the following section. In addition, all properties, whose field dependencies will be analyzed in the subsequent four chapters, are defined in this section.

### A. Zero magnetic field

The main conclusions from the anomalies of the thermal expansion coefficient at $T_{SP}$ in zero magnetic field have already been presented in a previous publication [14]. From general thermodynamic arguments an anomaly of $\alpha$ is expected for each phase transition with a finite pressure dependence of the transition temperature. This yields not only for mean field jumps, where the anomalies of $\alpha$ and the specific heat $C_p$ are related via the Ehrenfest relation, but also for phase transitions strongly affected by fluctuations [42] as the spin–Peierls transition in $CuGeO_3$ [14,32]. Assuming a finite pressure dependence of $T_{SP}$ one expects the same temperature dependence of the leading singular parts of $C_p$ and $\alpha$ at the phase transition. Quantitatively both quantities are related by a scaling factor measuring the (positive or negative) uniaxial pressure dependence of the transition temperature. Thus, as long as one treats the anomalies of the thermal expansion coefficient ($\Delta\alpha$) and the specific heat ($\Delta C$) in a similar way, one can determine the uniaxial pressure dependence of the transition temperature in the limit of vanishing pressure. The relationship reads

$$\left.\frac{\partial T_{SP}}{\partial p}\right|_{p\to 0} = V_m T_{SP} \cdot \frac{\Delta\alpha}{\Delta C}\,, \tag{1}$$

where $V_m$ denotes the volume per mol. Experimentally it is found that in $CuGeO_3$ the similarity between $C_p$ and $\alpha$ is restricted to a very narrow temperature range $|T_{SP}-T| \lesssim 0.2K$,

where sample inhomogeneities may strongly alter the temperature dependence. Therefore it is not possible to extract the critical behavior of the specific heat in $CuGeO_3$ [32] from the thermal expansion data. Nevertheless, Eq. 1 is valid for $CuGeO_3$, since the hydrostatic pressure dependence calculated from the thermal expansion and specific heat [14] perfectly agrees with the hydrostatic pressure dependence that is directly determined via susceptibility measurements at finite pressures [43].

To obtain a quantitative measure of the anomaly size we consider the largest deviation of the measured thermal expansion from the extrapolated behavior above $T_{SP}$ ($\alpha_{extr.}$, solid line in Fig. 1) $\Delta\alpha \equiv \max(\alpha(T < T_{SP}) - \alpha_{extr.})$, i.e. the height of the asymmetric peaklike anomaly. Note that $\Delta\alpha$ does not correspond to a real jump of $\alpha$ in the sense of a mean field theory. Below $T_{SP}$ the anomalous contribution to $\alpha$, i.e. the difference between the measured and extrapolated temperature dependence $\delta\alpha(T) \equiv \alpha(T) - \alpha_{extr.}(T)$, strongly differs from that of the specific heat. This is found experimentally, but also expected from e.g. CF theory. $C(T < T_{SP})$ is dominated by the magnetic excitations and therefore shows activated behavior at low temperatures [44,32,33], whereas $\delta\alpha$ is closely related to the structural order parameter (Q), i.e. the dimerization of the lattice. By definition it measures the development of a spontaneous strain ($\epsilon$) in the D phase [14–16].

To describe the temperature dependence of $\epsilon$ and $\delta\alpha$ and their relationship to Q one can start from the usual Ginzburg–Landau expansion of the free energy. Taking the expression given by Cross and Fisher [3], adding the elastic energy $1/2c\epsilon^2$ (c = elastic constant) and assuming a coupling between dimerization and lattice strains $\mu Q^2\epsilon$ ($\mu$ = const.), which is quite common for structural phase transitions [45], the free energy reads:

$$F = \gamma\left[1 - \frac{T}{T_{SP}} - \frac{1}{2}\eta\left(\frac{H}{T_{SP}}\right)^2\right]Q^2 + \frac{1}{2}\nu Q^4 + \mu Q^2\epsilon + \frac{1}{2}c\epsilon^2 \qquad (2)$$

The constants $\gamma$, $\eta$, and $\nu$ are related to the mean field thermodynamic properties below $T_{SP}$ and the leading order of the decrease of $T_{SP}$ in magnetic fields [3]. In thermodynamic equilibrium without external stress, i.e. for $\frac{\partial F}{\partial \epsilon} = 0$, it is easy to obtain the relationship between $\epsilon$ and the order parameter from Eq. 2. The spontaneous strain is proportional to the square of the order parameter [14,16] and thus the anomalous contribution of the thermal expansion represents the temperature derivative of $Q^2$:

$$Q^2(T) = -\frac{c}{\mu}\epsilon(T) \equiv -\frac{c}{\mu}\cdot\int_{T_{SP}}^{T}\delta\alpha(T')dT' \qquad (3)$$

In Fig. 6 we show that in zero field the scaling between the spontaneous strain obtained from the thermal expansion coefficient and the intensity of a superstructure reflection from neutron scattering data [46] is fulfilled in the entire temperature range below $T_{SP}$ (see also Ref. [16]). The intensity of the superstructure reflection is proportional to the square of the dimerization, i.e. of the structural order parameter. Moreover, it is apparent from Fig. 6 that the thermal expansion yields a high resolution measurement of $Q^2(T)$, since the scatter of these data is much smaller than that of the diffraction experiments.

At this point we mention that it is also possible to determine the temperature dependence of the spin–Peierls order parameter in external fields from Equ. 3. In this case one has to define the anomalous contribution of $\alpha$ with respect to the extrapolated behaviour of $\alpha$

measured in the corresponding field. For quite general reasons a finite field dependence of $\alpha$ in the U phase, i.e. a finite magnetostriction, is expected due to the magnetoelastic coupling which is a precondition for the occurrence of a spin–Peierls transition. This magnetoelastic coupling also implies a magnetic field dependence of $\alpha_{\rm extr.}$. However, in our analysis of $Q(T, H)$ which we will present in the subsequent sections we will neglect this field dependence of $\alpha_{\rm extr.}$ for two reasons.

First, as shown in Fig. 1 the field dependence of $\alpha$ in the U phase is extremely small (not resolvable). Note that this does not contradict a finite magnetostriction, since the magnetic part of $\alpha$ does not scale with the magnetostriction itself but with its temperature dependence, which is very weak in the U phase as mentioned in section III B. Second, although $\alpha_{\rm extr.}$ is not known exactly, it is apparent from Fig. 1 that it is much smaller than the anomalous contribution $\delta\alpha$. Thus, any reasonable choice of the background as a function of temperature and field yields the same anomalous contribution $\delta\alpha$ within our resolution. Therefore in the following we will assume a field independent $\alpha_{\rm extr.}$. Up to now there are only few diffraction data of $CuGeO_3$ in magnetic fields available to check our assumption. The Inset of Fig. 6 compares the spontaneous strain in a field of 10 Tesla to the intensity of a superstructure reflection in a field of 9.85 Tesla [46]. Although there are small differences in the fields as well as their orientations with respect to the crystal axes the agreement of the data is quite good. We mention that the same scaling factor was used for comparing the zero field and field data, respectively.

Let us now turn to the discussion of the temperature dependence of the spin–Peierls order parameter in zero field. In Fig. 7 we compare the experimentally determined $Q^2(T)/Q^2(0K)$ to a theoretical BCS temperature dependence (dotted line), which has been found for other spin–Peierls compounds [47]. Obviously, there are strong deviations in the entire temperature range below $T_{SP}$ for $CuGeO_3$. For $T \to T_{SP}$ this is of course due to the fluctuations of the order parameter. As a further consequence of these fluctuations the transition temperature is reduced compared to a hypothetical mean field transition temperature ($T_{SP}^{mf}$). Since the mean field temperature dependence of Q depends on $T_{SP}$ the fluctuations may also explain the deviations between the measured $Q^2(T)$ and the dotted line in Fig. 7 at low temperatures. Vice versa, assuming a BCS mean field temperature dependence at low temperatures one can estimate the decrease of the transition temperature due to fluctuations. A corresponding analysis is shown in Fig. 7. Below about 10K the experimentally found $Q^2(T)$ follows a BCS temperature dependence with a $T_{SP}^{mf} \simeq 15.8$K, i.e. $(T_{SP}^{mf} - T_{SP})/T_{SP}^{mf} \simeq 10\%$. Although there is a large uncertainty and in addition to that no real physical meaning of $T_{SP}^{mf}$, we emphasize that a quantitative comparison to mean field theories has in principle to consider a decrease of $T_{SP}$ which is due to fluctuations.

Close but not too close to the phase transition the temperature dependence of the spontaneous strain is well described by a power law $\epsilon \propto (T_{SP} - T)^{2\beta_\epsilon}$ (Fig. 7, see also Ref. [14,48]). From a fit to our data we find $2\beta_\epsilon = 0.61(5)$. The large error in the exponent is a direct consequence of the uncertainty in the absolute value of $T_{SP}$ discussed above. Renormalization group theory predicts an exponent $\beta = 0.325$ for the order parameter of the three dimensional structural transition in $CuGeO_3$ (universality class 3d Ising). This prediction is confirmed by our data when assuming the scaling between $\epsilon$ and $Q^2$ (see Eq. 3). However, note that the large error bar of $2\beta_\epsilon$ prevents a further discrimination between different three dimensional universality classes (XY, Heisenberg). Moreover, deviations from the power law

behavior of the spontaneous strain occur very close to $T_{SP}$. This is only partially due to sample inhomogeneities, since such deviations are also expected for a more general reason. As mentioned above the critical behavior of the thermal expansion coefficient for temperatures very close to $T_{SP}$ is expected to scale with that of the specific heat. Therefore the critical behavior of $\epsilon = \int \delta\alpha$ should change very close to $T_{SP}$ and finite values of $\int \delta\alpha$ above $T_{SP}$ are expected.

In the following four sections we will investigate the field dependence of the quantities defined above, i.e. the field dependence of:
(i) the anomaly size $\Delta\alpha$,
(ii) the critical exponent $2\beta_\epsilon$,
(iii) the spontaneous strain $\epsilon$, and
(iv) the temperature dependence of the order parameter Q.

### B. Field dependence of $\Delta\alpha$

As can already be inferred from Figs. 1 and 2, the size of the anomalies of $\alpha$ markedly decreases as a function of H. In Fig. 8 $\Delta\alpha$ is plotted as a function of the magnetic field. The correlation between this field dependence of $\Delta\alpha$ and the phase diagram is apparent. A dramatic change of $\Delta\alpha$ occurs exactly at the field, where the character of the phase transition changes. Therefore a clear discrimination between U/D and U/I transitions is possible, when considering the temperature dependence of the lattice constants. Furthermore, our data indicate significant structural differences between the D and I phases. The much smaller anomalies of $\alpha$ at the U/I transitions mean that the spontaneous strain in the I phase is strongly reduced compared to that in the D phase (see below). Besides this pronounced change of $\Delta\alpha$(H) at the tricritical point the data in Fig. 8 also show a smaller decrease of $|\Delta\alpha|$ with increasing field for both U/D and U/I transitions. Although we could follow the latter only within a restricted field range, our data suggest a rather strong field dependence of $\Delta\alpha$ at the U/I phase boundary, which amounts to about 5%/Tesla. This rather strong decrease, which occurs at a roughly constant $T_{SP}$, indicates the presence of continuous structural changes within the I phase as a function of H.

At the U/D phase boundary we find a much weaker field dependence of $\Delta\alpha$, though the transition temperature decreases stronger. Up to H = 12.15 Tesla the reduction of $\Delta\alpha$ amounts only to about 10%. Note that the decrease of $|\Delta\alpha|$ obtained in the entire field range of U/D transitions is much smaller than the decrease of the specific heat anomaly found for a rather small field of 6 Tesla [32]. Moreover, as visible in Fig. 8 $|\Delta\alpha|$ shows a nonlinear decrease with increasing field similar to that of the transition temperature $T_{SP}$(H). Indeed the decreases of both quantities can empirically be related to each other. The ratio $\Delta\alpha/\sqrt{T_{SP}(H)}$ (right part of Fig. 8) is a constant value for all magnetic fields, i.e. $\Delta\alpha(H) \propto \sqrt{T_{SP}(H)}$.

The size of the anomaly of $\alpha$ is related to the (uniaxial) pressure dependence of $T_{SP}$ (Eq. 1.), which strongly differs for different spin–Peierls compounds [2]. Thus, $\Delta\alpha$ itself is not predicted by theory. However, the field dependence of $\Delta\alpha$ can be compared – at least qualitatively – to theoretical predictions. The universal H–T phase diagram of spin–Peierls compounds implies a similar universality for a single compound when studied at

finite pressure. This is valid at least in the limit of vanishing pressure, which is sufficient to discuss our data. A pressure induced change of $T_{SP}(H = 0T)$ also affects the scaling of the field axis in the phase diagram. To take this into account $\partial T_{SP}/\partial p$ has to change as a function of H:

$$\left.\frac{\partial T_{SP}(H,p)}{\partial p}\right|_{p\to 0} = \left.\frac{\partial T_{SP}(0,p)}{\partial p}\right|_{p\to 0} \cdot \left(\frac{T_{SP}(H)}{T_{SP}(0)} - \frac{H}{T_{SP}(0)} \cdot \frac{\partial (T_{SP}(H))}{\partial H}\right) \tag{4}$$

$$\simeq \left.\frac{\partial T_{SP}(0,p)}{\partial p}\right|_{p\to 0} \cdot \left(1 + \tau \frac{g^2 H^2}{4 T_{SP}^2(0)}\right) (\text{for } \; H \leq 6T) \tag{5}$$

Note that the expression in the brackets of Eq. 5, which is derived from the quadratic decrease of $T_{SP}(H)$ (see section IV), is larger than 1. This means that the absolute value of the pressure dependence of $T_{SP}$ increases with increasing magnetic field. Combining Eq. 1 and 4 the field dependence of $\Delta\alpha$ is given by:

$$\frac{\Delta\alpha(H)}{\Delta\alpha(0)} = \frac{\Delta C(H)}{\Delta C(0)} \cdot \left(1 - \frac{H}{T_{SP}(H)} \cdot \frac{\partial (T_{SP}(H))}{\partial H}\right) \tag{6}$$

It is apparent from this equation that one expects a rather small change of $\Delta\alpha$ as a function of the magnetic field. Especially, the decrease of the relative anomaly size $\Delta\alpha(H)/\Delta\alpha(0)$ is expected to be much weaker than that of the specific heat. However, a detailed knowledge of the field dependence of the specific heat is necessary to analyze the simple scaling we find between $\sqrt{T_{SP}}$ and $\Delta\alpha$ (Fig. 8). Simple models for $\Delta C(H)$, e.g. based on the free energy given in [3], are not sufficient. Assuming a mean field behavior $\Delta C(H) \propto T_{SP}(H)$ one even obtains an increase of $|\Delta\alpha|$ with increasing field, which is in disagreement with the data. Studies of the specific heat in high magnetic fields are in progress and a detailed comparison of $\Delta C(H)$ and $\Delta\alpha(H)$ obtained at the same crystal will be given in a forthcoming publication. At present we conclude that the rather small field dependence of $\Delta\alpha$ for fields below 12 Tesla shown in Fig. 8 is in qualitative agreement with the field dependence estimated from thermodynamic relations.

### C. Critical behavior of the spontaneous strain in external fields

In zero magnetic field the spontaneous strain $\epsilon$ close to $T_{SP}$ follows a power law expected for the squared order parameter (see Fig. 7). In Fig. 9 we show $\epsilon$ as a function of the reduced temperature $1 - T/T_{SP}(H)$ for several magnetic fields in a double logarithmic scale. From these plots a power law behavior in a rather field independent temperature range $0.7 < T/T_{SP} < 0.95$ is found for all fields studied except those very close to the tricritical point, where two transitions occur (see Fig. 3). Moreover, it is apparent from Fig. 9 that for low magnetic fields the slope in the double logarithmic scale is roughly constant, i.e. the exponent $2\beta_\epsilon$ is constant. There is, however, a pronounced difference between the low field data and those at 15 and 16 Tesla, where a smaller exponent is present.

The field dependence of $2\beta_\epsilon$ is plotted in the lower part of Fig. 9. As mentioned above and displayed in the figure there is a rather large systematic error ($\pm 0.05$) of the absolute values due to the uncertainty in the absolute value of $T_{SP}$ at a given field. This uncertainty does, however, not affect the field dependence of $2\beta_\epsilon$, since the field induced decrease of

$T_{SP}$ is extractable with much higher accuracy from our data. In other words, an alternative definition of $T_{SP}$ in zero magnetic field causes a shift of $2\beta_\epsilon$ to higher or lower values, but the field dependence of $2\beta_\epsilon$ shown in the lower part of Fig. 9 remains nearly unchanged. For the U/D transitions at low fields a large exponent of about 0.6 is found, which decreases only slightly with increasing field. Within the error this value is consistent with that expected for a 3d Ising transition ($\beta = 0.325$) as discussed for the zero field data.

The critical exponents of the U/I transitions are significantly smaller than those of the U/D transitions and show a rather strong increase with increasing magnetic field. The interpretation of the findings for the U/I transition is more complicated for two reasons. First the nature of the I phase is still discussed controversially [9] and there are to our knowledge no theoretical predictions for the critical exponents. Second our studies are restricted to a field range rather close to the tricritical point where theory predicts a smaller exponent $\beta = 0.25$. This proximity might be the reason for the systematic increase of $2\beta_\epsilon$ with increasing field and thus, one may argue that the small exponents we observe for all U/I transitions are related to tricritical behavior. However, above $H_c$ the range of small $2\beta_\epsilon$ is much larger than below $H_c$ (Fig. 9). This pronounced difference indicates a critical behavior within the I phase, which differs from the rather usual one found at the U/D transitions. In principle the small values of $2\beta_\epsilon$ might also arise from a different strain order parameter coupling in the I phase. However, as we will show below, the temperature dependence of the spontaneous strain for high fields indicates the usual linear quadratic coupling for the U/I transitions, too. Irrespective of whether the critical behavior at the U/I transition is intrinsically characterized by a smaller $\beta_\epsilon$ or the tricritical behavior is found in a larger field range, the critical exponents indicate a qualitative difference between the D and I phases.

### D. Magnetic field dependence of the spontaneous strain

From our data of the thermal expansion coefficient in magnetic fields we can follow the spontaneous strain as a function of magnetic field as well as a function of temperature. Fig. 10 presents the development of the spontaneous strain as a function of H and T. In addition, we show the spontaneous strain as a function of temperature for some representative fields in Fig. 11. The magnetic field dependence of $\epsilon$ is dominated by the field induced phase transitions. At low temperatures there is only a moderate decrease of $\epsilon$ with increasing field within the D phase, i.e. for $H \lesssim 12$T. At the discontinuous D/I transition a strong decrease of $\epsilon$ occurs in a narrow field range followed by a weaker decrease within the I phase. Close to the D/I boundary the temperature dependence of $\epsilon$ reflects the competition between these phases leading to multiple transitions.

The field dependence of $\epsilon$ at fixed temperatures is closely related to the field dependence of the lattice constant, i.e. to our measurements of the magnetostriction presented in section III. However, small but significant differences occur, when comparing the field dependence of the lattice constant $a$ quantitatively with $\epsilon$. The field dependence of $\epsilon$ is always smaller than the magnetostriction at the same temperature (see Figs. 4 and 11). These differences arise from the finite magnetostriction above $T_{SP}$. Whereas the spontaneous strain is zero and thus field independent above $T_{SP}$, the lattice constant does depend on the magnetic field. From the definition of the spontaneous strain one obtains:

$$\epsilon(\mathrm{H,T}) - \epsilon(\mathrm{O,T}) = \int_{T_0 > T_{SP}}^{T} (\delta\alpha(H,T')dT' - \delta\alpha(0,T'))dT' = \frac{\Delta L(H,T)}{L} - \frac{\Delta L(H,T_0)}{L} \quad (7)$$

Eq. 7 means that the field dependence of $\epsilon$ at a temperature T is given by the difference of the magnetostriction at the same temperature and the magnetostriction at a temperature $T_0$ above $T_{SP}$. Subtracting the magnetostriction data at $T_0 = 20$K from the low temperature magnetostriction leads to a good agreement between the spontaneous strain derived from the magnetostriction and thermal expansion data, respectively. That means that the lattice constant and the spontaneous strain follow variations of T and H in a reversible way in almost the entire field and temperature range. The only exception is a small region around the D/I phase boundary at low temperatures where hysteresis effects are present in the magnetostriction.

Please note that the need for correcting the magnetostriction data before comparing with $\epsilon$ does not imply that the magnetostrictive effects present in the U phase are also relevant in the dimerized phase. The correction according to Eq.7 is just a consequence of the definition of the spontaneous strain. There is, however, some experimental evidence for an unexpected magnetoelastic coupling in the D phase. A closer inspection of the magnetostriction data in Fig. 4 below about 5K shows a small increase of $a$ with increasing field in the D phase. Since the sign of this effect differs from the magnetostriction found at the field driven transitions, it is probably not related to the field dependence of the spontaneous strain. However, there seems to be a correlation to the magnetostriction in the U phase, which shows the same sign and order of magnitude. At present we have no explanation of this finite magnetostriction in the dimerized phase at low temperatures. Detailed investigations of the other lattice constants and also for crystals with different impurity concentrations are in progress to clarify this low temperature behavior.

A detailed discussion of the temperature dependence of Q in external fields will be given in the following section. Here we will restrict the discussion of $\epsilon(H)$ to the low temperature range, i.e. for $T \to 0$. Within the D phase the scaling between the spin–Peierls order parameter and the spontaneous strain is valid as discussed in section V A. Thus, it is apparent from Fig. 11 that the field dependence of the order parameter at low temperatures is extremely weak. Extrapolating the data to $T = 0$ our measurements are consistent with a field independent $Q^2(0)$. In other words, not only the wave vector of the distortion is pinned and thus field independent up to the critical field $H_{D/I}$ but also the amount of the structural distortion for $T \to 0$ does not change as a function of H. This is in striking contrast to the strong decrease of the energy gap in the magnetic excitations due to the Zeeman splitting of the triplet state [37]. The scaling between structural deformation Q and the energy gap, theoretically expected and observed in $CuGeO_3$ for zero magnetic field [16,49], is obviously not present at finite fields. However, we emphasize that this is not in contrast to theoretical treatments of the spin–Peierls transition. For example, calculations within the XY model really yield a field independent order parameter at $T = 0$ [50].

A similar simple interpretation of $\epsilon$(H) as a measure of the amount of the structural distortion is not possible at and above the D/I phase transition. The spontaneous strain for an individual field is a consequence of the strain order parameter coupling, too. According to our data $\epsilon$ is reduced but still large for the U/I transitions. However, in contrast to the behavior at low fields the character of the lattice distortion now changes as a function of

H. This has been studied with x–ray diffraction showing a field dependent wave vector $q$ of the lattice distortion at and slightly above the D/I transition [9]. In this field range it is impossible to correlate the field dependence of the spontaneous strain to a single quantity. Assuming a homogeneous incommensurate modulation of the lattice the decrease of the spontaneous strain may be a consequence of a reduced amplitude of the distortion and/or a consequence of a wave vector dependent strain order parameter coupling. Similarly, assuming a domain–wall picture, the decrease of $\epsilon$ may be a consequence of a reduced amplitude of the distortion within the individual domains and/or the number of domain walls. With the present knowledge of the structural deformation in the I phase it seems neither possible to favor one of the two models nor to relate the $\epsilon$(H) to a structural characteristic of the I phase. However, note that the large anomalies at the D/I transition clearly show structural differences between the D and I phases. Moreover, as visible in Fig. 11 and also in the magnetostriction data, there is no indication for a field independent $\epsilon$ for $T \to 0$ as we observe within the D phase. Obviously the structural parameter(s) determining the spontaneous strain in the I phase continuously change with increasing field.

### E. Temperature dependence of the spin–Peierls order parameter in external fields

The field dependencies of the quantities discussed in the last three subsections, $\Delta\alpha(\mathrm{T_{SP}})$, $2\beta_\epsilon$, and $\epsilon(\mathrm{T} = \text{const.})$, mainly reflect the field driven phase transitions. In particular, there are only minor changes within the D phase. A completely different picture is obtained when considering the temperature dependence of the order parameter. Within the D phase the temperature dependence of $\epsilon$ well below $\mathrm{T_{SP}}$ systematically increases with increasing field (see Fig. 11). For fields of 15 and 16 Tesla, i.e. in the I phase, a much smaller slope is obtained. In order to analyse the temperature dependencies of the (squared) order parameter we will not consider the spontaneous strains plotted in Figs. 10 and 11. Instead of that we will directly investigate their temperature derivatives $\delta\alpha$, where small changes of the temperature dependence of $\mathrm{Q}^2$ show up more clearly.

As a starting point of this discussion we investigate the field dependence of $\delta\alpha$ in the low temperature range. Fig. 12(a) shows $\delta\alpha$ at a fixed temperature of 5K as a function of magnetic field. It is apparent that this field dependence strongly differs from those discussed in the last sections. In particular, it strongly differs from the field dependence of the anomaly size $\Delta\alpha$ at $\mathrm{T_{SP}}$. Within the D–phase $|\delta\alpha|$ systematically increases with H. At the D/I boundary $|\delta\alpha(5\mathrm{K})|$ jumps back to smaller values and for higher fields it is roughly constant. We emphasize that this strong field dependence of $\delta\alpha(5\mathrm{K})$ in the D phase is not due to the decreasing $\mathrm{T_{SP}}$(H). As displayed in Fig. 12(b) at a fixed reduced temperature ($\mathrm{T_{SP}}/2$) a very similar field dependence of $\delta\alpha$ is present in the D phase. However, in this representation $|\delta\alpha|$ is significantly smaller in the I phase than in the D phase. This difference can be traced back to the different sizes of the anomalies at $\mathrm{T_{SP}}$ (see Fig. 8). In Fig. 12(c) the different sizes are taken into account by considering relative values, i.e. $\delta\alpha(T_{SP}/2)$ / $\Delta\alpha$, as a function of H. The result is rather surprising. The zero field value roughly coincides with the values at very high magnetic fields, i.e. with those of the I phase. However, the pronounced field dependence of $\delta\alpha$ within the D is still present.

In the following we first analyze $\mathrm{Q}^2$(T) for different magnetic fields within the D phase. In order to avoid complications due to tricritical behavior and the additional anomalies in

the vicinity of the D/I phase boundary (see Fig. 3) we restrict the discussion to fields below 11 Tesla. From the data analysis given in the previous sections one concludes that the decrease of the transition temperature is the main consequence of the magnetic field in this field range, whereas only minor changes occur in all structural quantities. In particular, the zero temperature value of $Q^2$ as well as its critical behavior are roughly field independent. Thus, one might even expect a universal relationship between the order parameter and the reduced temperature $t = (T_{SP}(H) - T) \; / \; T_{SP}(H)$ within the D phase, i.e. a simple scaling behavior $Q(t, H) = Q(t, 0)$.

However, this universality is not present at all in the D phase. To demonstrate this we consider $\delta\alpha \cdot T_{SP}(H)$, i.e. the derivative $\partial\epsilon(t)/\partial t \propto \partial Q^2(t)/\partial t$ (Fig. 13). Obviously there are pronounced systematic differences of the temperature dependence of Q in different magnetic fields. Close to the transition temperature $\partial Q^2(t)/\partial t$ decreases with H, whereas at low temperatures the opposite field dependence is present. At $t \simeq 0.44$ all curves meet in a single point, i.e. $\partial Q^2(t)/\partial t$ is field independent for this particular reduced temperature. It is not possible to improve the agreement between the curves for different magnetic fields in the whole temperature range by any normalization of $\delta\alpha$ (see inset of Fig. 13). For example, when investigating $Q^2(t)$ divided by its zero temperature value, i.e. the quantity shown for the zero field data in Fig. 7, a systematic increase of the derivative with H is obtained at low temperatures. Thus, the BCS–like low temperature behavior of Q(T) present for H = 0 (see Fig. 7) does significantly change with increasing magnetic field.

Instead of a field independent Q(t) we empirically find a – to our opinion – rather surprising result. The temperature dependence of the order parameter in different magnetic fields is universal on an *absolute* temperature scale. Fig. 14 shows a plot of $\delta\alpha/\sqrt{T_{SP}(H)}$ versus $(T - T_{SP}(H))$: All the curves from 0 up to 11 Tesla, i.e. in the entire field range of the dimerized phase, perfectly agree within the experimental resolution. Note that the factor $1/\sqrt{T_{SP}(H)}$, which is used to scale the y–axis, is necessary to take into account the slight decrease of the anomaly size $\Delta\alpha$. We emphasize that the temperature axis for the different curves in Fig. 14 is not scaled but simply shifted by the field dependent transition temperature. To our knowledge there is no theoretical calculation of the temperature dependence of the spin–Peierls order parameter in magnetic fields, at least none that is consistent with our findings. For example from the exact solution of the XY–model one obtains indeed an increase of $\partial Q^2/\partial t$ with H at low temperatures. However, the opposite field dependencies for small and large reduced temperatures as well as the crossing at $t \simeq 0.44$ are not obtained [50].

Now we turn to the temperature dependence of the spontaneous strain in the I phase, which compares well with that in zero magnetic field. At first sight any similarity between high field and zero field data is covered by the much smaller size of the anomalies at the U/I transition. However, the data in Fig. 12 already give a first hint on this similarity: After normalizing the $\delta\alpha$ axis the temperature derivatives of the spontaneous strains at high fields nearly agree with that in zero field at $T_{SP}/2$ (Fig. 12c). This holds at $T_{SP}/2$ but also in the entire low temperature range. On reduced scales the temperature dependencies of $\delta\alpha$ in H = 0 and H = 16T are very similar (see Fig. 15). Only close to $T_{SP}$ slight differences are present, which have already been discussed in connection with the critical exponent $2\beta_\epsilon$ (see Fig. 9). The scaling used to obtain agreement between H= 0 and H = 16 T data is quite natural, since the first – considering the reduced temperature $T_{SP}/2$ – takes into account the

smaller $T_{SP}$ and the second the reduced anomaly size $\Delta\alpha$ and/or the reduced spontaneous strain in the I phase (see Figs. 8 and 11). From Fig. 15 one thus concludes that apart from the absolute values of both $\epsilon(T = 0)$ and $T_{SP}$ the spontaneous strain in the incommensurate phase corresponds to that found in the D phase at $H = 0$. This similarity is also found for the other fields with U/I transitions.

To connect $\epsilon$ in the I phase to the order parameter of the incommensurate modulation, we can follow the procedure applied for $H = 0$. A strain order parameter coupling causes a spontaneous strain and the temperature dependence of $\epsilon$ measures that of the incommensurate modulation (Eq. 2 and 3). There are no neutron scattering measurements of the superstructure reflections. Thus, we can not prove a linear quadratic coupling, as we did for smaller fields in Fig. 6. However, the similarity between zero and high magnetic fields strongly indicates the same linear quadratic strain order parameter coupling in the I phase. This means that the spontaneous strain yields a measure of the squared order parameter of the I phase, too. In particular, at low temperatures the order parameter of the I phase follows roughly a BCS mean field behavior (see Fig. 7). Up to now there are – to our knowledge – neither measurements nor calculations of Q(T) in the I phase of any spin–Peierls compound. Thus, at present we can neither compare our result to other findings nor judge whether the presented data give a possibility to distinguish between the different models of the structural distortion in the I phase, i.e. domain walls or sinusoidal modulation.

## VI. CONCLUSIONS

Using a high resolution capacitance dilatometer we have investigated structural and thermodynamic properties of the inorganic spin–Peierls compound $CuGeO_3$. The temperature and field dependence of the lattice constant $a$ have been studied via measurements of the thermal expansion and the magnetostricton, respectively. Pronounced anomalies are found at all phase transitions present in the characteristic field temperature phase diagram of spin–Peierls compounds. Thus, clear structural differences between the three phases are established from our data. The very large anomalies we observe at all phase transitions allow for a precise determination of the H–T phase diagram of $CuGeO_3$. Moreover, our data show that all phase boundaries strongly depend on pressure, since the anomalies of the thermal expansion and the magnetostriction are related to the uniaxial pressure dependencies of the transition temperature and field, respectively. Summarizing our detailed comparison of the experimental H–T phase diagram to existing theories, one concludes that there are pronounced discrepancies to the soliton theory. On the other hand the predictions given by Cross as well as by Bulaevskii et al. are in rough agreement with the experimental results. This holds for the first order character of the D/I transition and also for a quantitative comparison of the transition fields at the phase boundaries. However, clear deviations from the latter theories are also present. The temperature at the tricritical point calculated by Bulaevskii et al., for instance, is significantly too small. With respect to this point the Cross theory agrees very well with the data. Moreover, the overall shape of the U/D phase boundary follows Cross' calculations although the field scales differ slightly. The "effective" field acting in $CuGeO_3$ is about 10% larger than predicted by theory. This enhancement indicates that particular magnetic properties of $CuGeO_3$ determine the exact positions of the phase boundaries.

Our high resolution measurements of the lattice constant do not only yield the phase boundaries. Properties of the ordered phase can also be extracted. From a simple treatment within Landau theory one obtains a scaling between the squared spin–Peierls order parameter and the spontaneous strain, which is experimentally confirmed for the U/D transitions. Since the anomalous contribution of the thermal expansion corresponds to the temperature derivative of the spontaneous strain, our data yield a high resolution measurement of the field and temperature dependence of the order parameter. The temperature dependence of the order parameter is strongly affected by fluctuations. In zero magnetic field, for example, there are pronounced deviations from a mean field behavior in the entire temperature range. Close to $T_{SP}$ a power law as a function of the reduced temperature is found and the extracted exponent is consistent with the predictions for a 3d–Ising transition. In order to describe $Q^2(T)$ at low temperatures by a BCS–like behavior one has to assume a 10% reduction of $T_{SP}$, which is due to fluctuations.

For the discussion of the field dependence of the spontaneous strain one has to discriminate between the different low temperature phases. Up to 12 Tesla $\epsilon(T, H)$ measures the dimerization, i.e. the order parameter of the D phase. There are three main conclusions from our data in this field range. At very low temperatures the order parameter is nearly field independent. The critical behavior at the U/D transition is also rather field independent for a wide field range. The third finding is rather surprising. The temperature dependence of $Q^2$ is universal on an absolute temperature scale, i.e. when plotting $Q^2$ versus $T_{SP}(H) - T$. In contrast pronounced systematic differences are present after scaling the temperature axes, i.e. when analyzing $Q^2$ as a function of the reduced temperature $\frac{T_{SP}(H)-T}{T_{SP}(H)}$. Thus, the similarity to a BCS–like behavior found for $H = 0$ rapidly vanishes with increasing field.

The interpretation of our findings involving the incommensurate phase is more complicated. In this field range the wave vector of the structural deformation changes with H and thus the spontaneous strain is not related to a single, i.e. field independent, structural parameter. The field dependence of $\epsilon$ might be a consequence of a field dependent order parameter as well as a field dependent strain order parameter coupling. Nevertheless, the temperature dependence of $\epsilon$ at a given field reflects that of the corresponding order parameter. At a fixed temperature, e.g. for $T \to 0$, there is a strong decrease of $\epsilon$ with increasing field. This decrease is most pronounced at the first order D/I transition itself, where $\epsilon$ reduces to about 40% of its zero field value. Within the I phase $\epsilon$ shows a further decrease with H, which indicates continuous structural changes as a function of field.

For fixed fields we analyzed the critical behavior of $\epsilon$ close to $T_{SP}$ as well as its temperature dependence well below the transition. The critical exponents in the I phase are significantly smaller than those found in the D phase. Although we could investigate the I phase only in a rather small field range, the critical exponents indicate a qualitative difference between U/D and U/I transitions. Apart from the region close to $T_{SP}$ the temperature dependence of $\epsilon$ in the I phase compares well with that of the squared order parameter for $H = 0$. Thus, the incommensurate lattice modulation roughly follows a BCS mean field behavior for $T \longrightarrow 0$, similar to the dimerization in zero magnetic field.

**Acknowledgements**

We are grateful to W. Brenig, E. Müller–Hartmann, and A. Klümper for stimulating discussion on many aspects of this work. We thank H. Micklitz and B. Sullewsky for critical

reading of the manuscript. A.R. and G.D. acknowledge NEDO for financial support. U.A. acknowledges support by the Graduiertenkolleg GRK14 of the Deutsche Forschungsgemeinschaft. This work was supported by the Deutsche Forschungsgemeinschaft through SFB 341.

# REFERENCES


[1] M. Hase, I. Terasaki and K. Uchinokura. *Phys. Rev. Lett.* **70**, 3651 (1993).

[2] J.W. Bray. In J.S. Miller, editor, *Extended Linear Chain Compounds,*. Plenum, New York 1983.

[3] M. Cross and D.S. Fisher. *Phys. Rev.* **B19**, 402 (1979).

[4] M.C. Cross. *Phys. Rev.* **B20**, 4606 (1979).

[5] M. Nishi, O. Fujita and J. Akimitsu. *Phys. Rev.* **B50**, 6508 (1994).

[6] G. Castilla, S. Chakravarty and V. J. Emery. *Phys. Rev. Lett.* **75**, 1823 (1995).

[7] J. Riera and A. Dobry. *Phys. Rev.* **B51**, 16098 (1995).

[8] B. Büchner, U. Ammerahl, T. Lorenz, W. Brenig, G. Dhalenne and A. Revcolevschi. *Phys. Rev. Lett.* **77**, 1624 (1996).

[9] V. Kiryukhin and B. Keimer. *Phys. Rev.* **B52**, R704 (1995).

[10] L.N. Bulaevskii, A.I. Buzdin and D.I. Khomskii. *Sol. State Commun.* **27**, 5 (1978).

[11] M. Fujita and K. Machida. *J. Phys. Soc. Japan* **53**, 4395 (1984).

[12] M. Hase, I. Terasaki, K. Uchinokura, M. Tokunaga, N. Miura and H. Obara. *Phys. Rev.* **B48**, 9616 (1993).

[13] The measurements of the thermal expansion coefficients along the $b$– and $c$–axis, respectively, will be presented in a forthcoming publication.

[14] H. Winkelmann, M. Braden, G. Dhalenne, A. Revcolevschi, E. Gamper and B. Büchner. *Phys. Rev.* **B51**, 12884 (1995).

[15] J.E. Lorenzo, H. Hirota, G. Shirane, J.M. Tranquada, M. Hase, K. Uchinokura, H. Kojima, I. Tanaka and Y. Shibuya. *Phys. Rev.* **B50**, 1278 (1994).

[16] Q. J. Harris, Q. Feng, R.J. Birgeneau, K. Hirota, K. Kakurai, J.E. Lorenzo, G. Shirane, M. Hase, K. Uchinokura, H. Kojima, I. Tanaka and Y. Shibuya. *Phys. Rev.* **B50**, 12606 (1994).

[17] M. Fujita, M. Arai, K. Ubukata, H. Ohta, M. Mino, M. Motokawa, K. Knight, R. Ibberson, J.B. Forsyth, S.M. Bennington, J. Akimitsu and O. Fujita. *Physica* **B219&220**, 95 (1996).

[18] A detailed discussion of the results of the magnetostriction measurements along the different crystal axes will be given in a forthcoming publication.

[19] A. Revcolevschi and G. Dhalenne. *Adv. Mater.* **5**, 9657 (1993).

[20] J.P. Pouget, L.P. Regnault, M. Ain, B. Hennion, J.P. Renard, P. Veillet, G. Dhalenne and A. Revcolevschi. *Phys. Rev. Lett.* **72**, 4037 (1994).

[21] R. Pott and R. Schefzyk. *J. Phys. E – Sci. Instrum.* **16**, 444 (1983).

[22] F.R. Kroeger and C.A. Swenson. *J. Appl. Phys.* **48**, 853 (1977).

[23] D. Bloch, J. Voiron, J.C. Bonner, J.W. Bray, I.S. Jacobs and L.V. Interrante. *Phys. Rev. Lett.* **44**, 294 (1980).

[24] D. Bloch, J. Voiron J.W. Bray, I.S. Jacobs, J.C. Bonner and J. Kommandeur. *Physics Lett.* **82A**, 21 (1981).

[25] V. Kiryukhin, B. Keimer and D.E. Moncton. *Phys. Rev. Lett.* **74**, 1669 (1995).

[26] M. Poirier, M. Castonguay, G. Dhalenne and A. Revcolevschi. *Phys. Rev.* **B51**, 6147 (1995).

[27] M. Saint-Paul, G. Reményi, N. Hegmann, P. Monceau, G. Dhalenne and A. Revcolevschi. *Phys. Rev.* **B52**, 15298 (1995).

[28] T. Hamamoto, G. Kido, M. Hase, Y. Sasago and K. Uchinokura. *Physica* **B201**, 171 (1994).
[29] R.K. Kremer. *Sol. State Commun.* **96**, 427 (1995).
[30] J.W. Bray. *Sol. State Commun.* **35**, 853 (1980).
[31] Y. Lépine. *Sol. State Commun.* **57**, 189 (1986).
[32] X. Liu, J. Wosnitza, H.v. Löhneysen and R.K. Kremer. *Z. Physik* **B98**, 163 (1995).
[33] S.B. Oseroff, S-W. Cheong, B. Aktas, M.F. Hundley, Z. Fisk and L.W. Rupp jr. *Phys. Rev. Lett.* **74**, 1450 (1995).
[34] J.C. Bonner, J.A. Northby, I.S. Jacobs and L.V. Interrante. *Phys. Rev.* **B35**, 1791 (1987).
[35] T. Nakano and H. Fukuyama. *J. Phys. Soc. Japan* **49**, 1679 (1980).
[36] T. Nakano and H. Fukuyama. *J. Phys. Soc. Japan* **50**, 2489 (1981).
[37] O. Fujita, J. Akimitsu, M. Nishi and K. Kakurai. *Phys. Rev. Lett.* **74**, 1677 (1995).
[38] H. Ohta, S. Imagawa, H. Ushiroyama, M. Motokawa, O. Fujita and J. Akimitsu. *J. Phys. Soc. Japan* **63**, 2870 (1994).
[39] J. Riera and S. Koval. *Phys. Rev.* **B53**, 770 (1996).
[40] J.A. Northby, H.A. Groenendijk, L.J. de Jongh, J.C. Bonner, I.S. Jacobs and L.V. Interrante. *Phys. Rev.* **B25**, 3215 (1982).
[41] M. Hase, I. Terasaki, Y. Sasago, K. Uchinokura, M. Tokunaga, N. Miura, G. Kido, T. Hamamoto and H. Obara. *Physica* **B201**, 167 (1994).
[42] A.B. Pippard. *Elements of classical thermodynamics*. University Press, Cambridge 1964.
[43] H. Takahashi, N. Môri, O. Fujita, J. Akimitsu and T. Matsumoto. *Sol. State Commun.* **95**, 817 (1995).
[44] S. Sahling, J.C. Lasjaunias, P. Monceau and A. Revcolevschi. *Sol. State Commun.* **92**, 423 (1994).
[45] A.D. Bruce and R.A. Cowley. *Structural phase transitions*. Taylor & Francis LTD, London 1981.
[46] L.P. Regnault, M. Ain, B. Hennion, G. Dhalenne and A. Revcolevschi. *Phys. Rev.* **B53**, 5579 (1996).
[47] D.E. Moncton, R.J. Birgeneau, L.V. Interrante and F. Wudl. *Phys. Rev. Lett.* **39**, 507 (1977).
[48] Q.J. Harris, Q. Feng, R.J. Birgeneau, K. Hirota, G. Shirane, M. Hase and K. Uchinokura. *Phys. Rev.* **B52**, 15420 (1995).
[49] M. Fujita, K. Ubukata, M. Arai, T. Tonegawa, M. Mino, M. Motokawa, K. Knight, B. Forsyth, S.M. Bennington, J. Akimitsu and O. Fujita. *Physica* **B219&220**, 95 (1996).
[50] E. Müller-Hartmann. private communication.

## FIGURES

FIG. 1. Thermal expansion of $CuGeO_3$ along the $a$–axis in different magnetic fields. The solid line represents the extrapolated low temperature behavior $\alpha_{\rm extr.}$ of the U phase.

FIG. 2. Thermal expansion of $CuGeO_3$ along the $a$–axis in different magnetic fields given in the figure. The curves are shifted by $5 \cdot 10^{-6}$/K for clarity.

FIG. 3. Thermal expansion of $CuGeO_3$ along the $a$–axis in magnetic fields close to the D/I phase boundary. The additional anomalies reflect temperature dependent transitions between the D and I phases and vice versa.

FIG. 4. Magnetostriction of $CuGeO_3$ along the $a$–axis at different temperatures given in the figure. Upper panel: Discontinuous transitions between D and I phases. With increasing T (indicated by the arrows) the character of the transition gradually changes from rather strong to weak first order.
Inset: Field derivatives $1/\mathrm{L} \cdot \partial \mathrm{L}/\partial \mathrm{H}$ at 3.4K measured with increasing ($\circ$) and decreasing ($\bullet$) magnetic field. The hysteresis, resolved up to $\sim$ 11K, systematically decreases with decreasing T.
Lower panel: Continuous transitions between D and U phases. The transition fields as well as the overall magnetostriction rapidly decreases with increasing T. Within the U phase (T=18K and T = 14K for H $\gtrsim$8T) a positive magnetostriction is present.

FIG. 5. Magnetic field temperature phase diagram of $CuGeO_3$ derived from thermal expansion (circles) and magnetostriction (triangles) data. The solid line shows the result of Cross' calculation. An almost perfect agreement to the experimental results for the entire U/D phase boundary is obtained by dividing the calculated field scale by 1.12 (dotted line, see text).
Inset: Hysteresis at the D/I phase boundary obtained from the magnetostriction measured with increasing (closed triangles) and decreasing field (open triangles).

FIG. 6. Comparison between the spontaneous strain ($\bullet$) and the intensity of a superstructure reflection ($\circ$) found from neutron diffraction [46]. Main part: Zero field data. Inset: Spontaneous strain in H = 10T and neutron scattering intensity in H = 9.85T.

FIG. 7. Symbols: Temperature dependence of the squared order parameter in zero magnetic field as obtained from the thermal expansion.
Solid line: Power law $((14.35 - \mathrm{T})^{0.61}$ representing the order parameter fluctuations close to $\mathrm{T_{SP}}$.
Dotted line: BCS mean field behavior for $\mathrm{T_{SP}} = 14.35$K.
Dashed line: BCS mean field behavior for a hypothetical $\mathrm{T_{SP}^{mf}} = 15.8$K (see text).

FIG. 8. Left panel: Anomaly size $\Delta\alpha \equiv \max(\alpha - \alpha_{\rm extr})$ as a function of magnetic field.
Right panel: $\Delta\alpha/\sqrt{\mathrm{T_{SP}}}$ versus magnetic field (see text).
The dashed vertical lines denote the field at the tricritical point.

FIG. 9. Critical behavior of $\epsilon$. Upper panel: $\epsilon$ versus reduced temperature on a double logarithmic scale. The curves are shifted for clarity.
Lower panel: Magnetic field dependence of the critical exponents $2\beta_\epsilon$.

FIG. 10. Spontaneous strain ($\circ$) as a function of temperature and magnetic field. The phase boundaries between the U, D, and I phases are given by the closed symbols ($\bullet$).

FIG. 11. Spontaneous strain as a function of T for several magnetic fields given in the figure. The different field ranges represent the different kinds of low temperature phases. At H=12.5 T the competition between D and I phase close to the D/I phase boundary is seen.

FIG. 12. Different representations of the temperature derivative $\delta\alpha = \partial\epsilon/\partial\mathrm{T} \propto \partial\mathrm{Q}^2/\partial\mathrm{t}$ of the spontaneous strain versus magnetic field:
a.): $\delta\alpha$(H) at a fixed temperature T = 5K.
b.): $\delta\alpha$(H) at a fixed reduced temperature $\mathrm{t} = \mathrm{T_{SP}(H)}/2$
c.): $-\delta\alpha/\Delta\alpha$ at $\mathrm{t} = \mathrm{T_{SP}(H)}/2$ (see text).

FIG. 13. Derivative $\delta\alpha \cdot T_{SP}(H) \propto \frac{\partial \mathrm{Q}^2(\mathrm{t})}{\partial \mathrm{t}}$ versus reduced temperatures t for different magnetic fields given in the figure. Inset: Same data after an arbitrary normalization of the y–axis.

FIG. 14. Universal temperature dependence of the D phase order parameter. Note, that the temperature axis is only shifted but not scaled by $\mathrm{T_{SP}(H)}$. The division of $\delta\alpha$ by $\sqrt{\mathrm{T_{SP}(H)}}$ takes into account the slight decrease of the anomaly size with H (see text).

FIG. 15. Comparison between the derivatives $\delta\alpha \cdot T_{SP}(H) \propto \frac{\partial \mathrm{Q}^2(\mathrm{t})}{\partial \mathrm{t}}$ versus reduced temperature t in H = 0 ($\circ$; left y–scale) and H = 16T ($\bullet$; right y–scale).

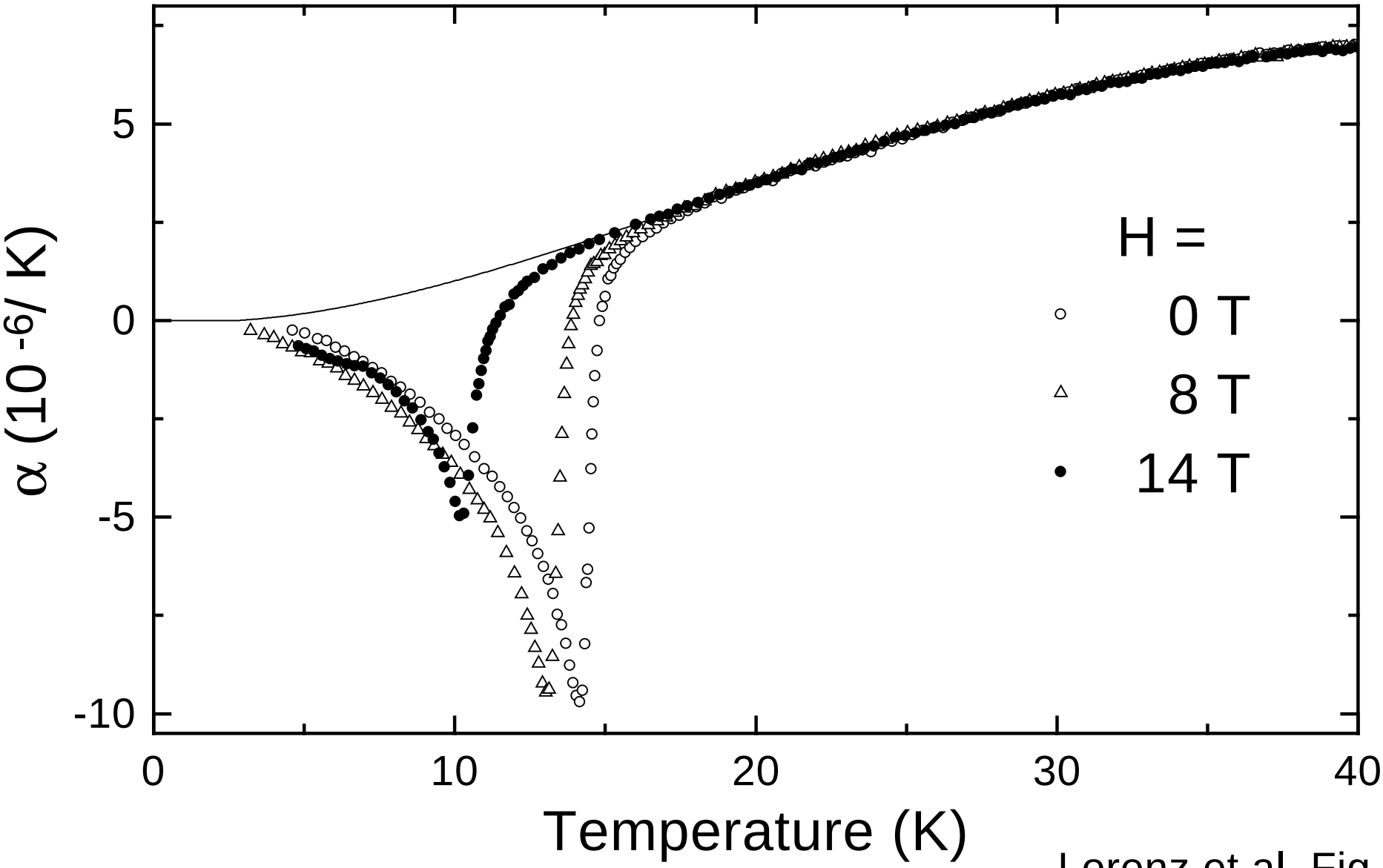


Lorenz et al. Fig. 1

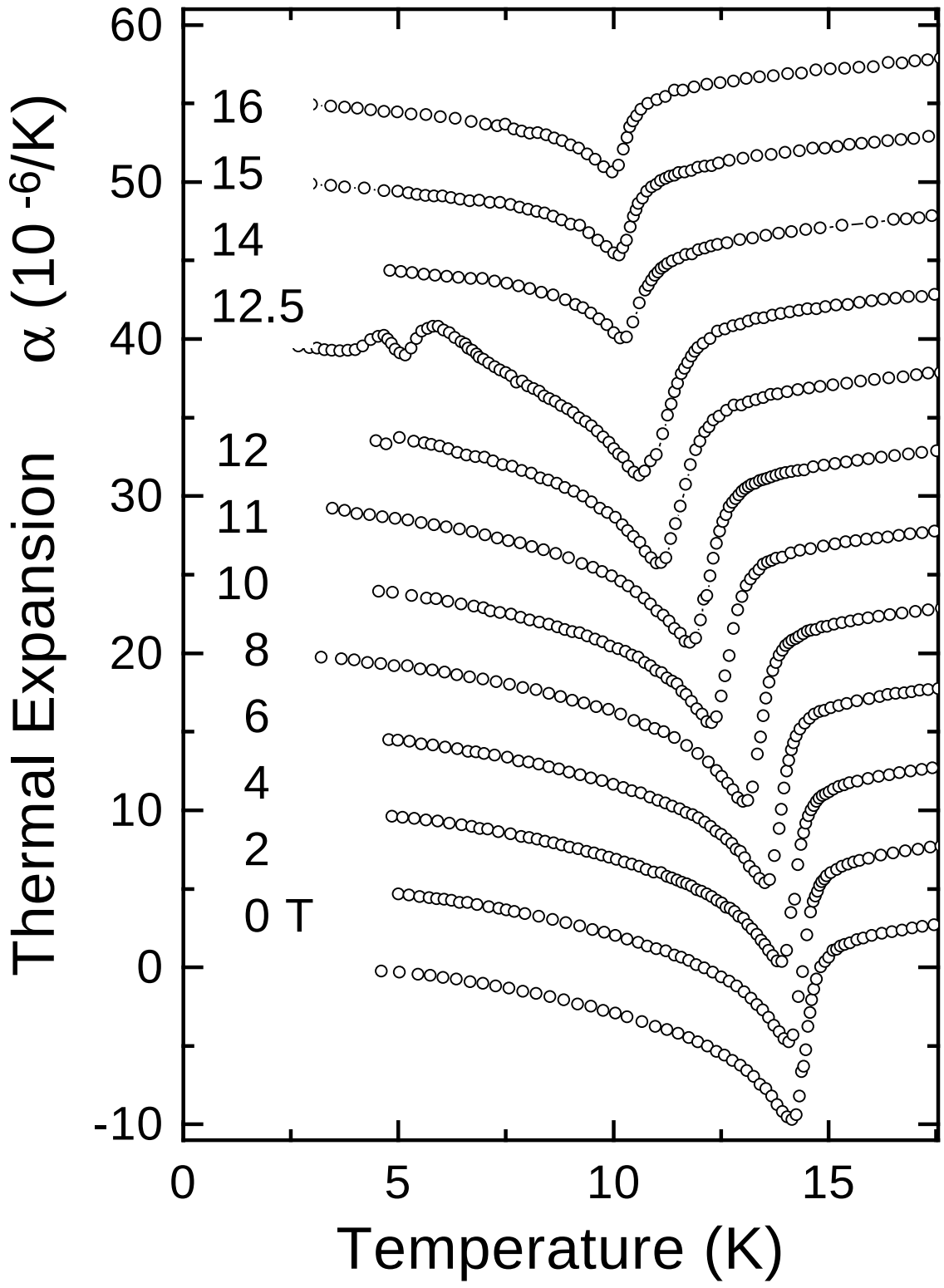


Lorenz et al. Fig. 2

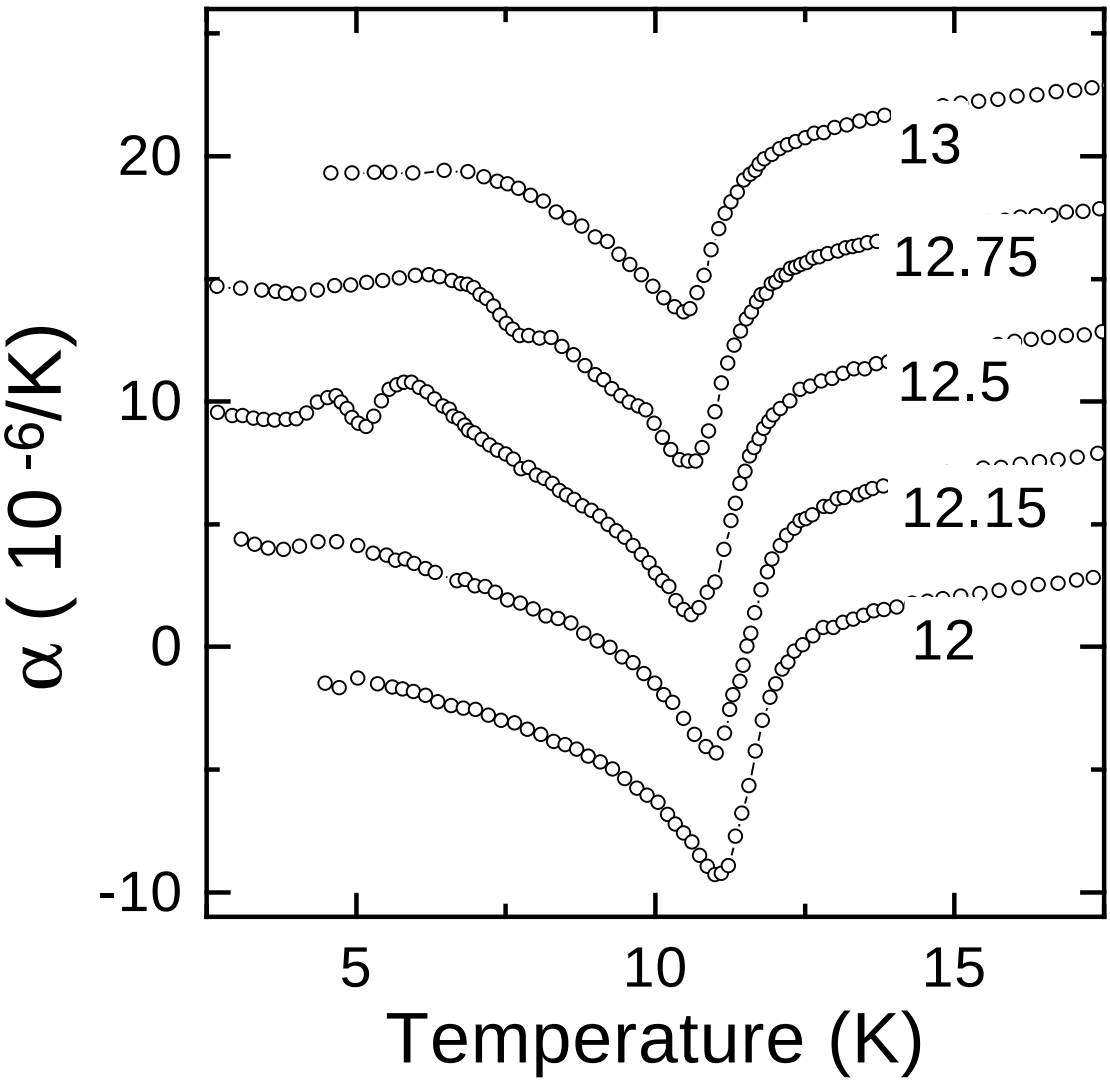


Lorenz et al. Fig. 3

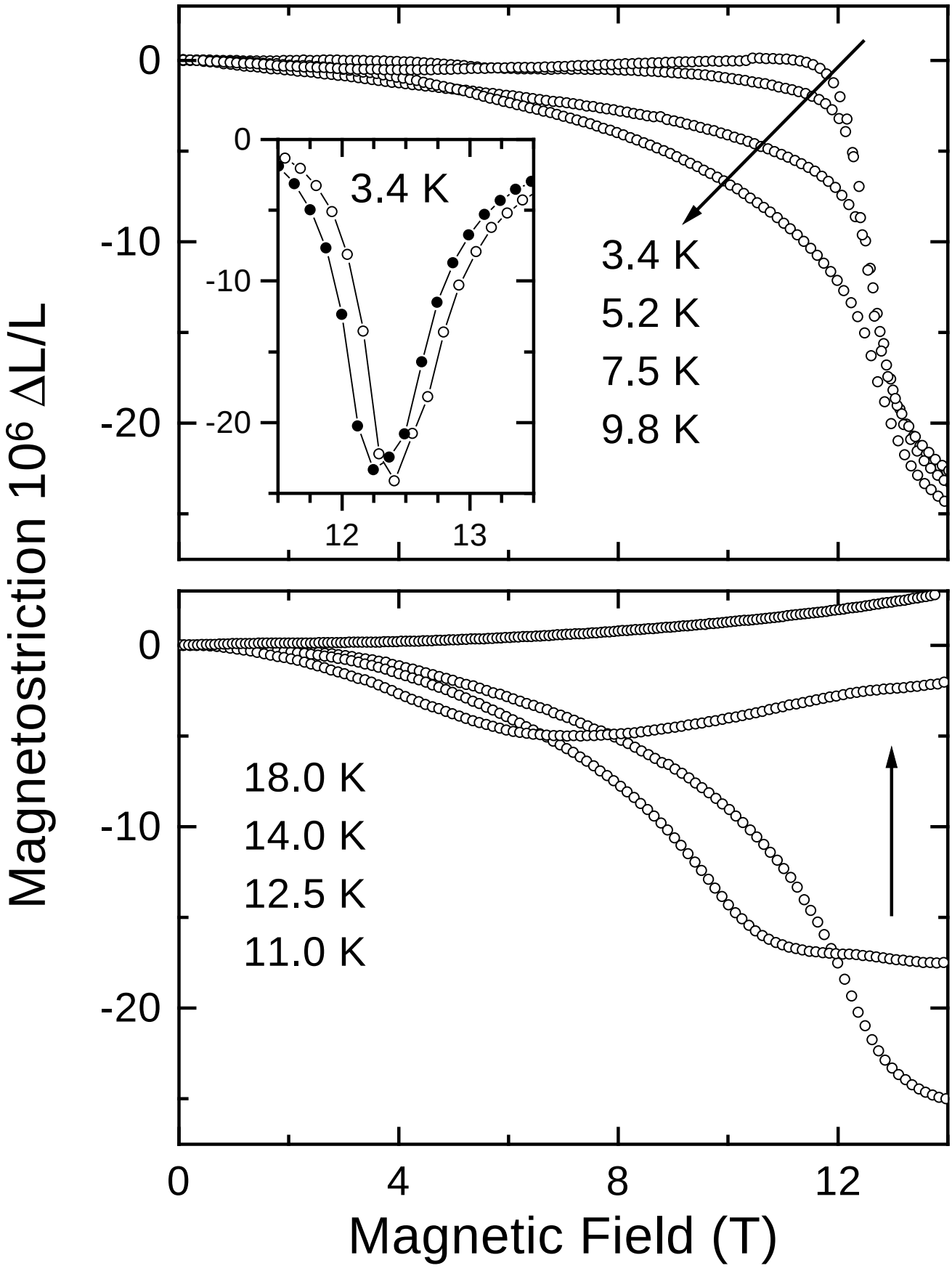


Lorenz et al. Fig. 4

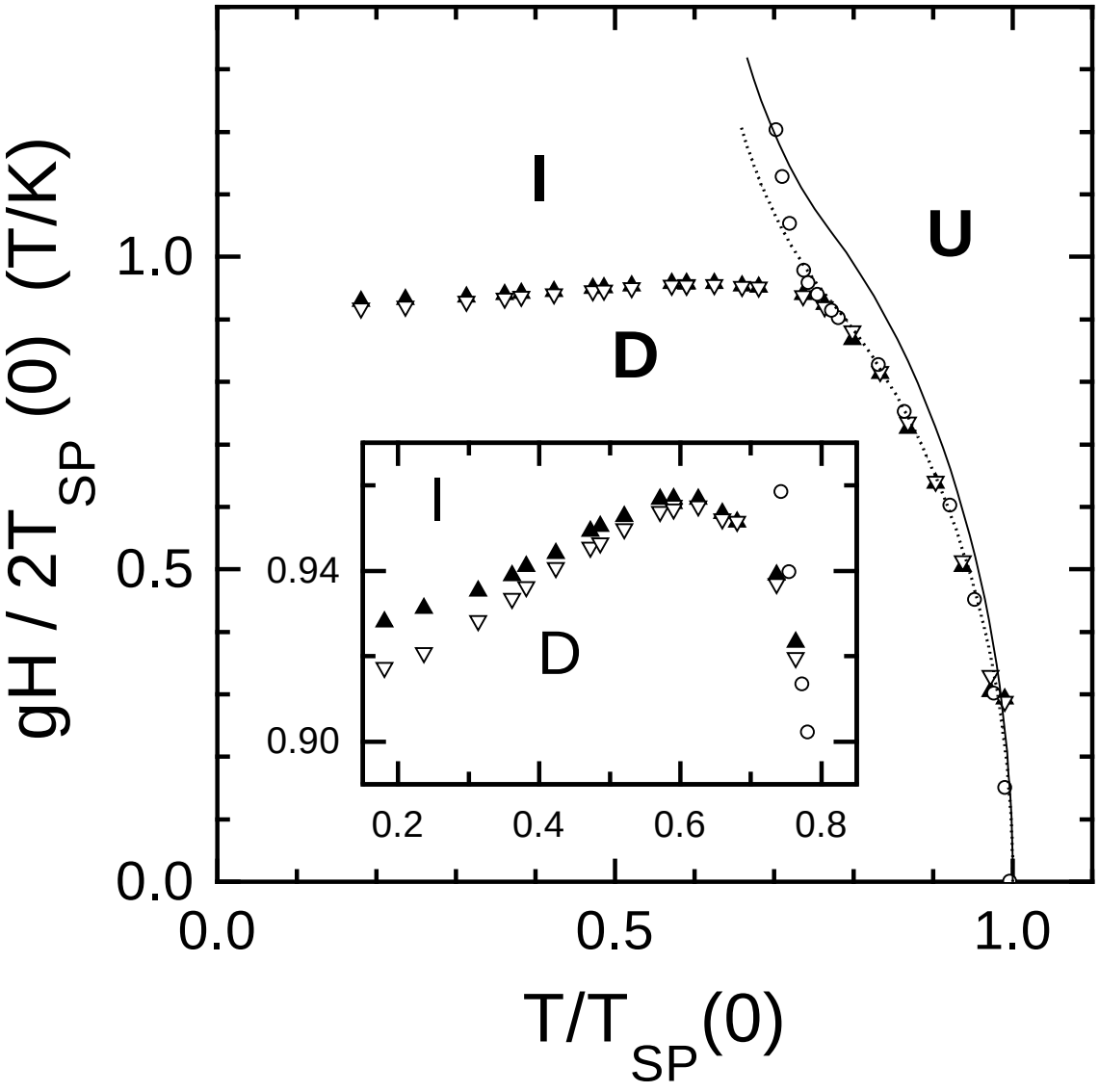


Lorenz et al. Fig. 5

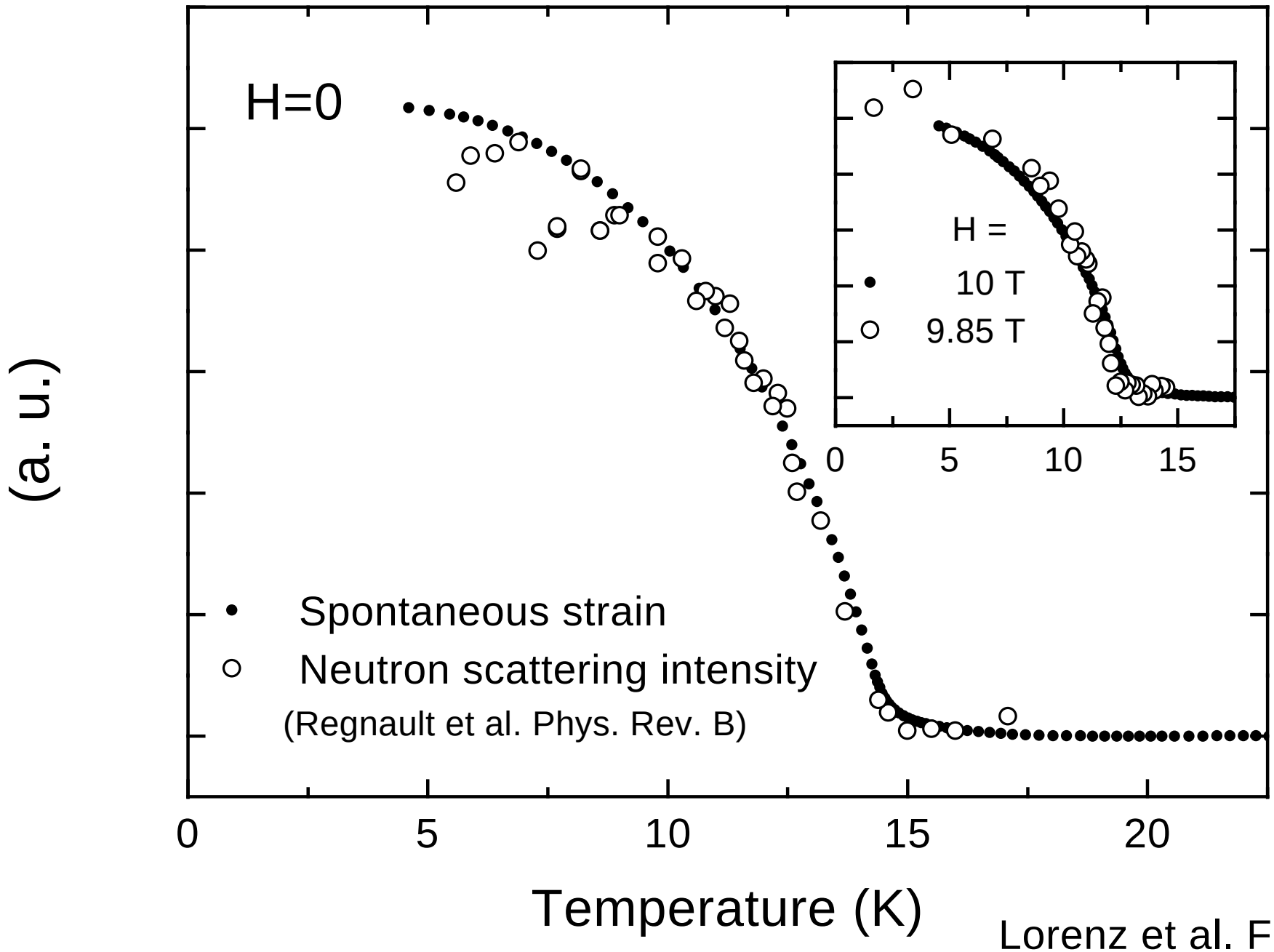


Lorenz et al. Fig. 6

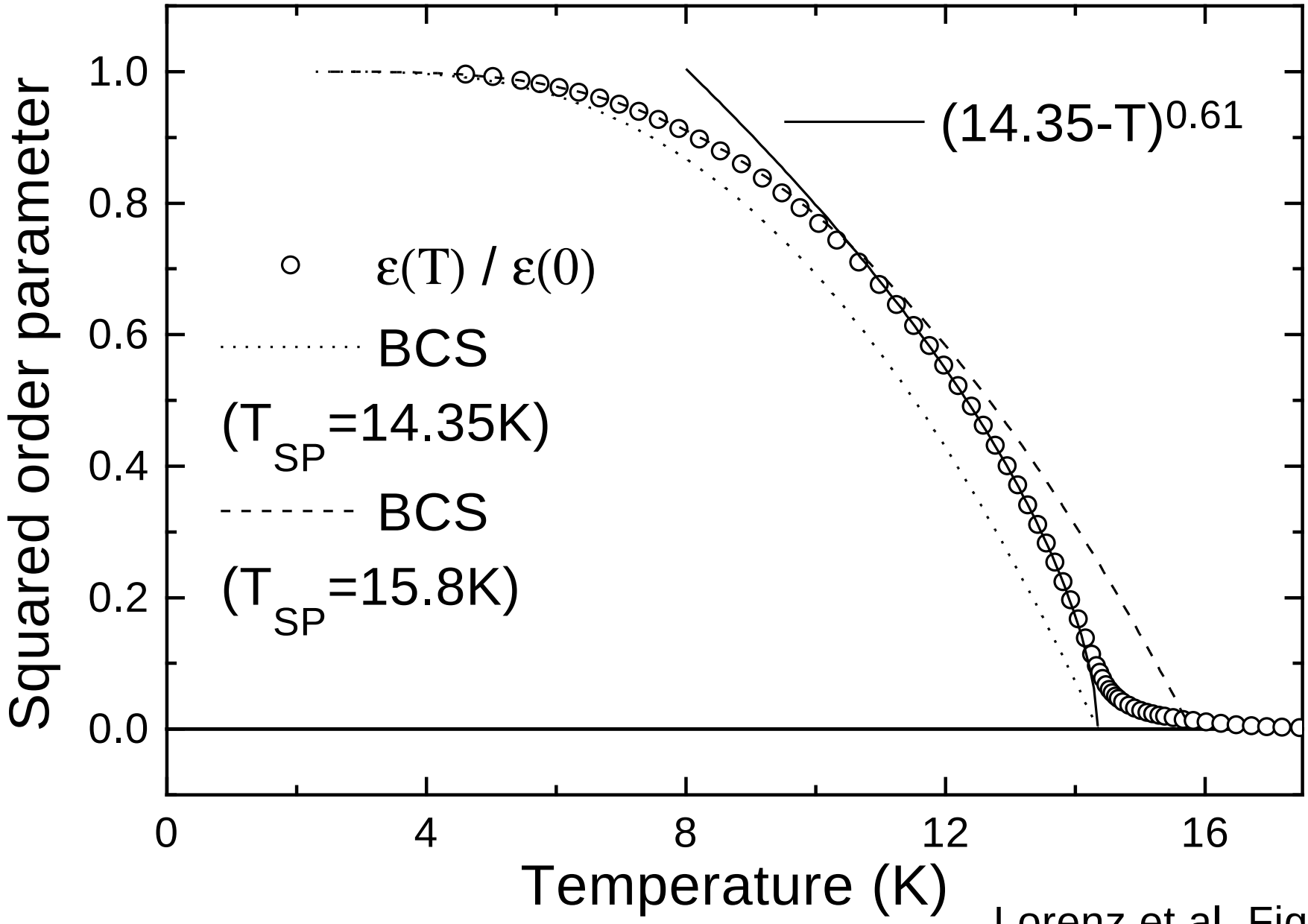


Lorenz et al. Fig. 7

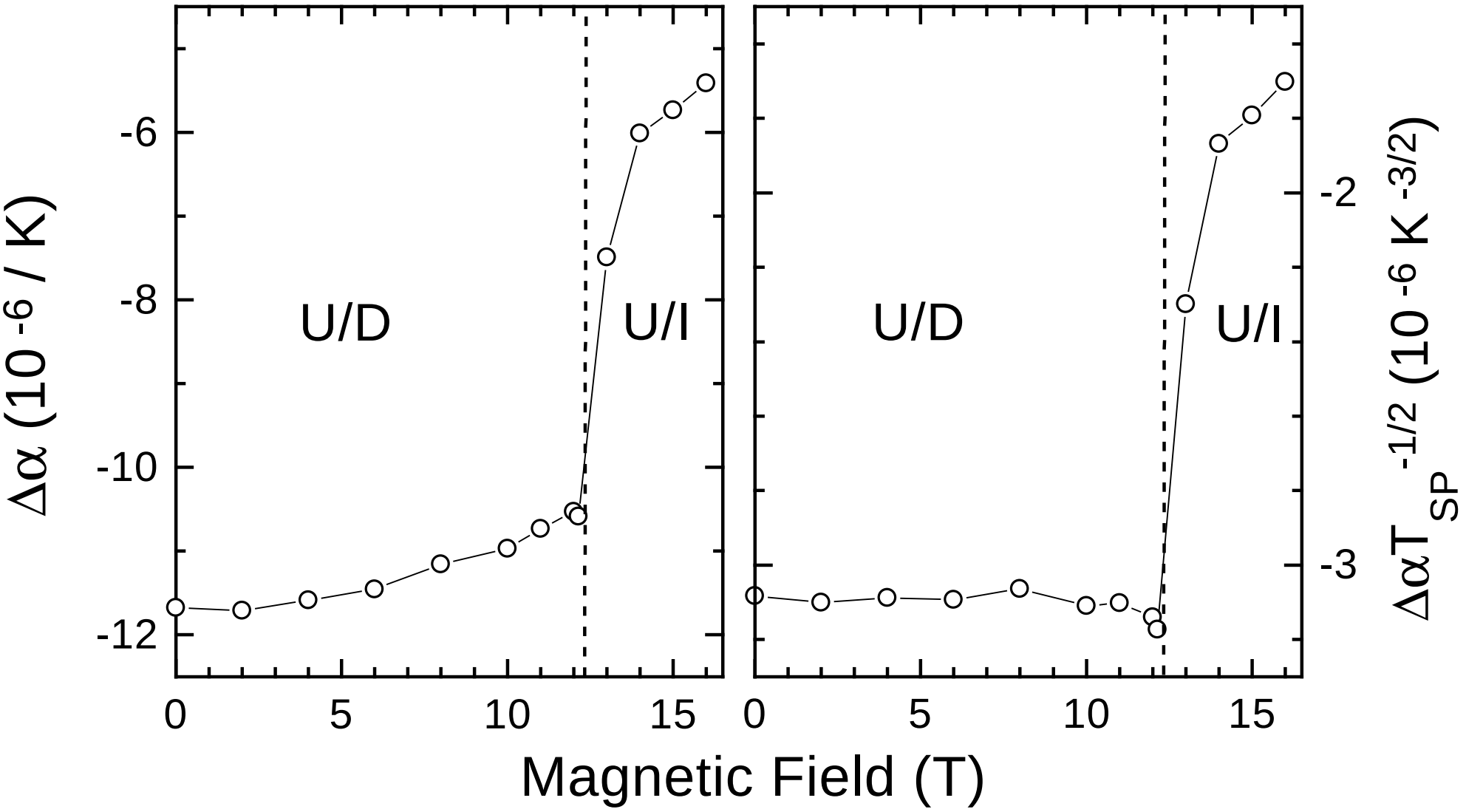


Lorenz et al. Fig. 8

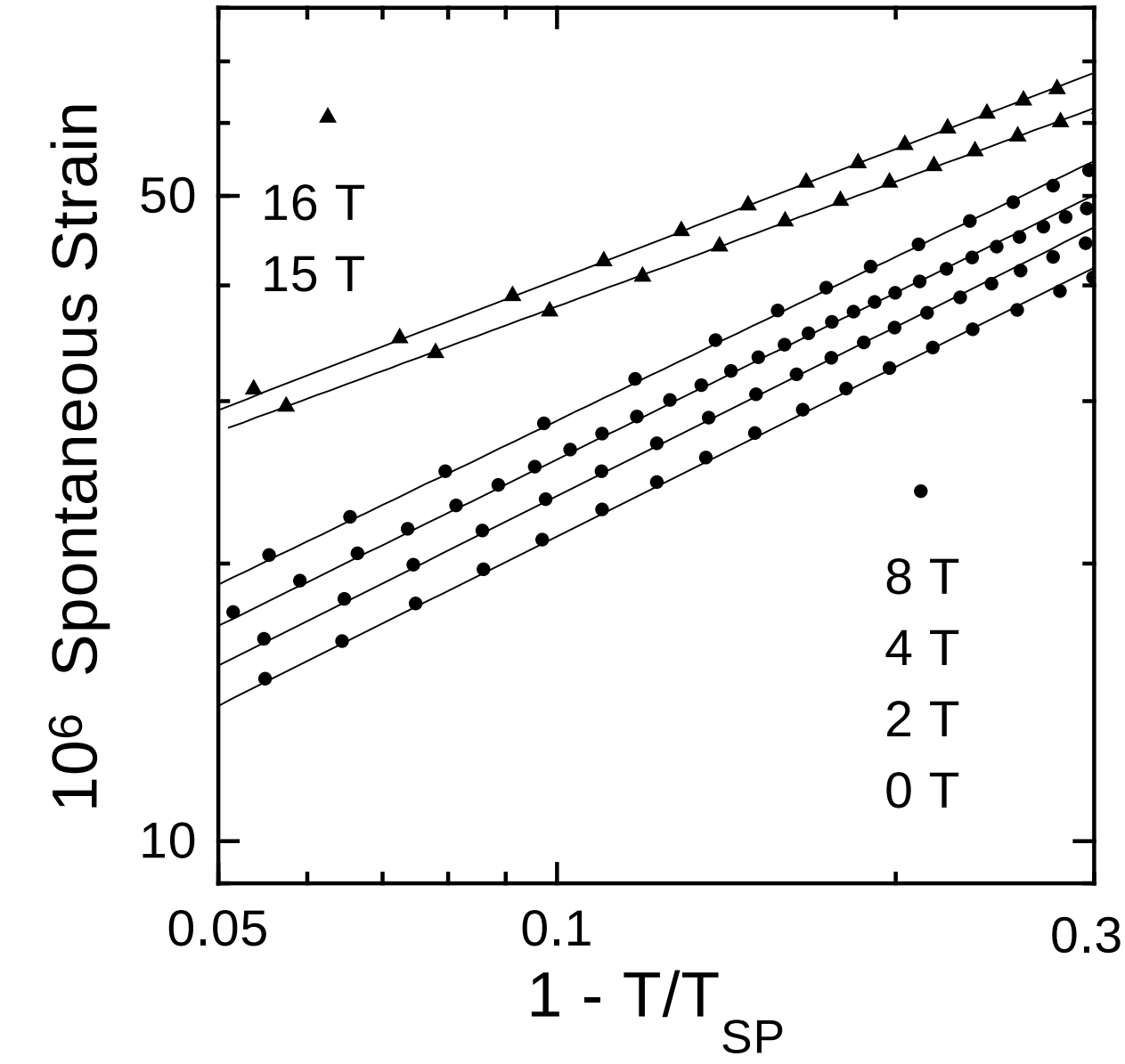


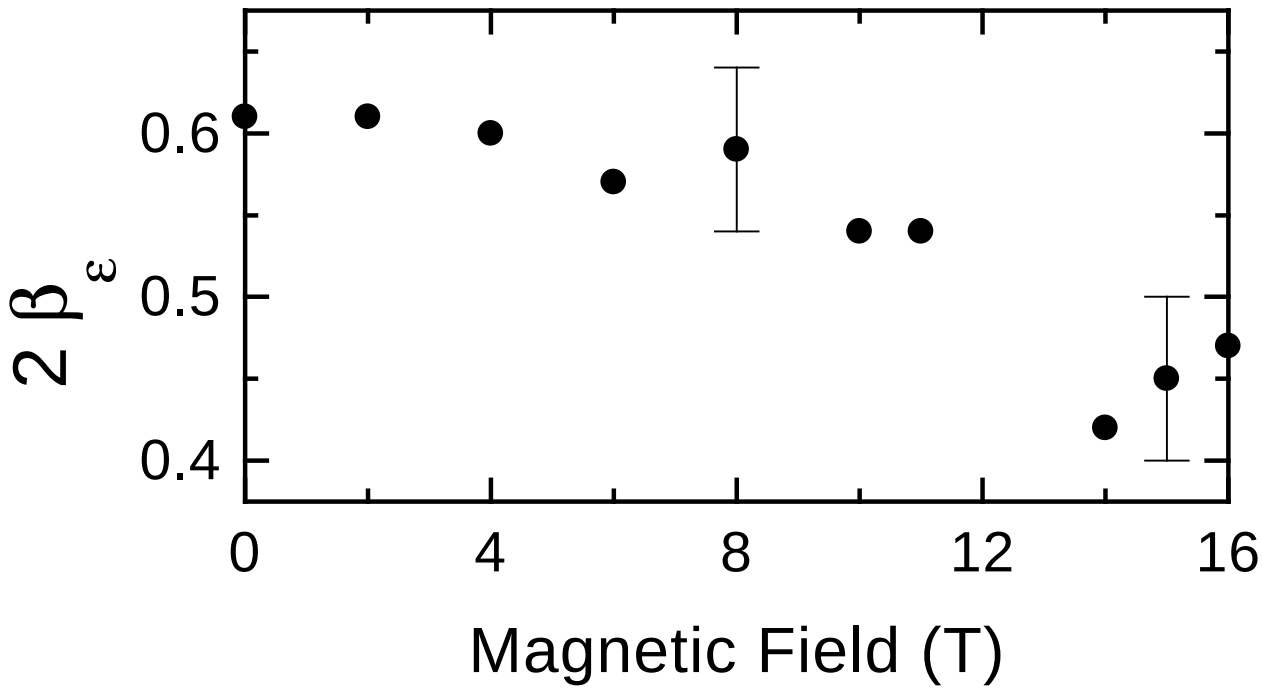


Lorenz et al. Fig. 9

This figure "fig10.gif" is available in "gif"  format from:

http://arXiv.org/ps/cond-mat/9610171v1

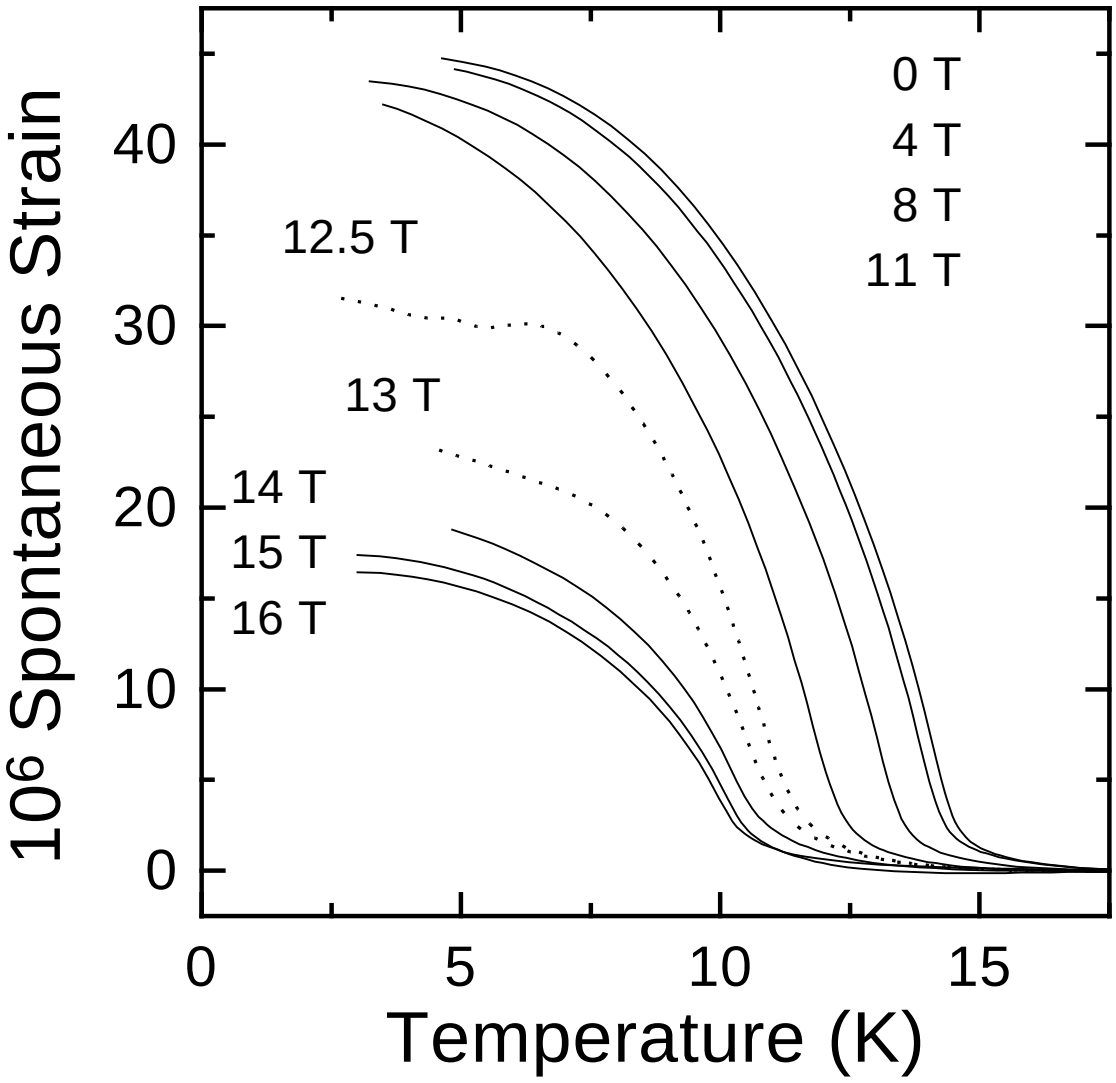


Lorenz et al. Fig. 11

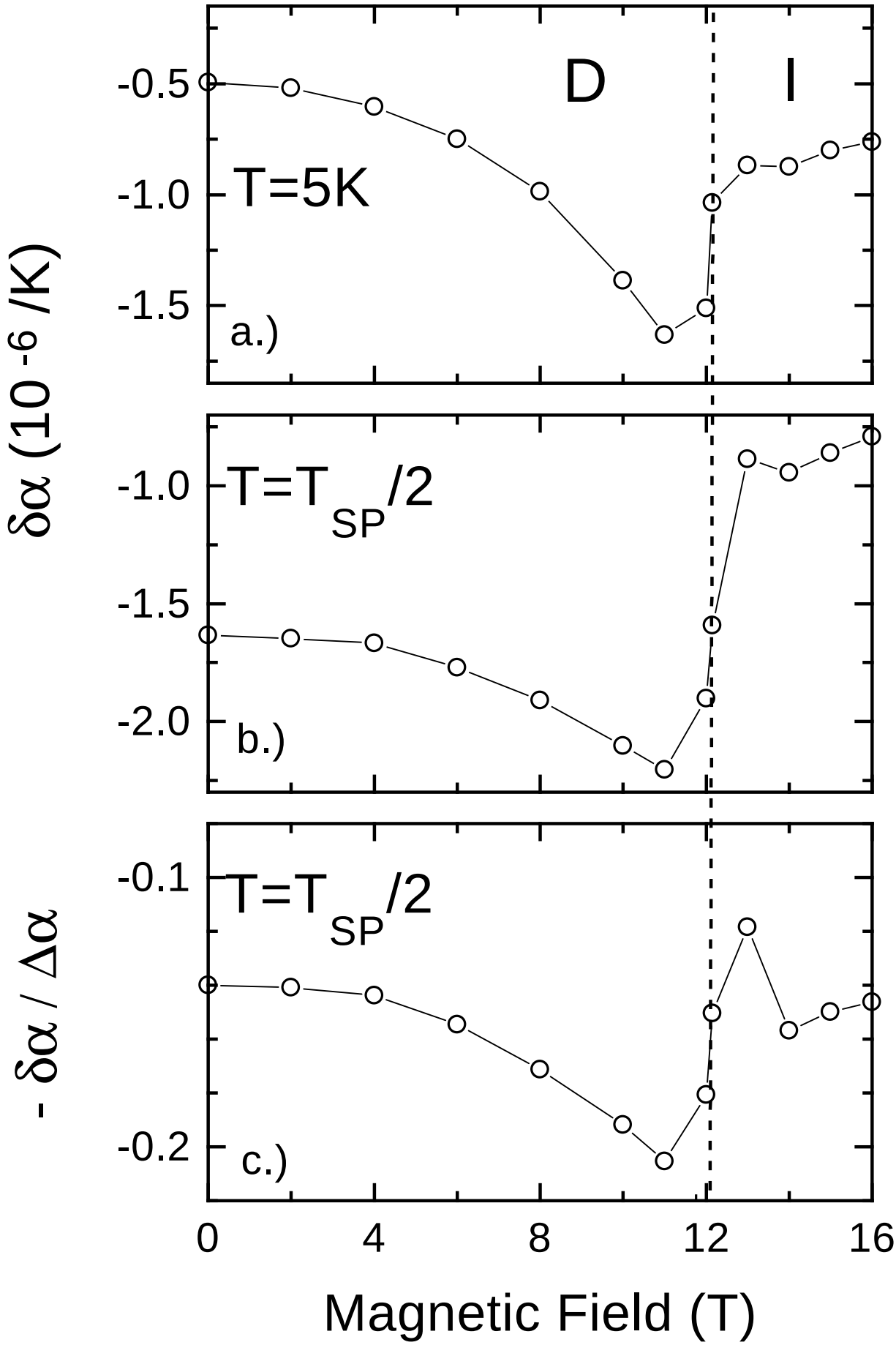


Lorenz et al. Fig. 12

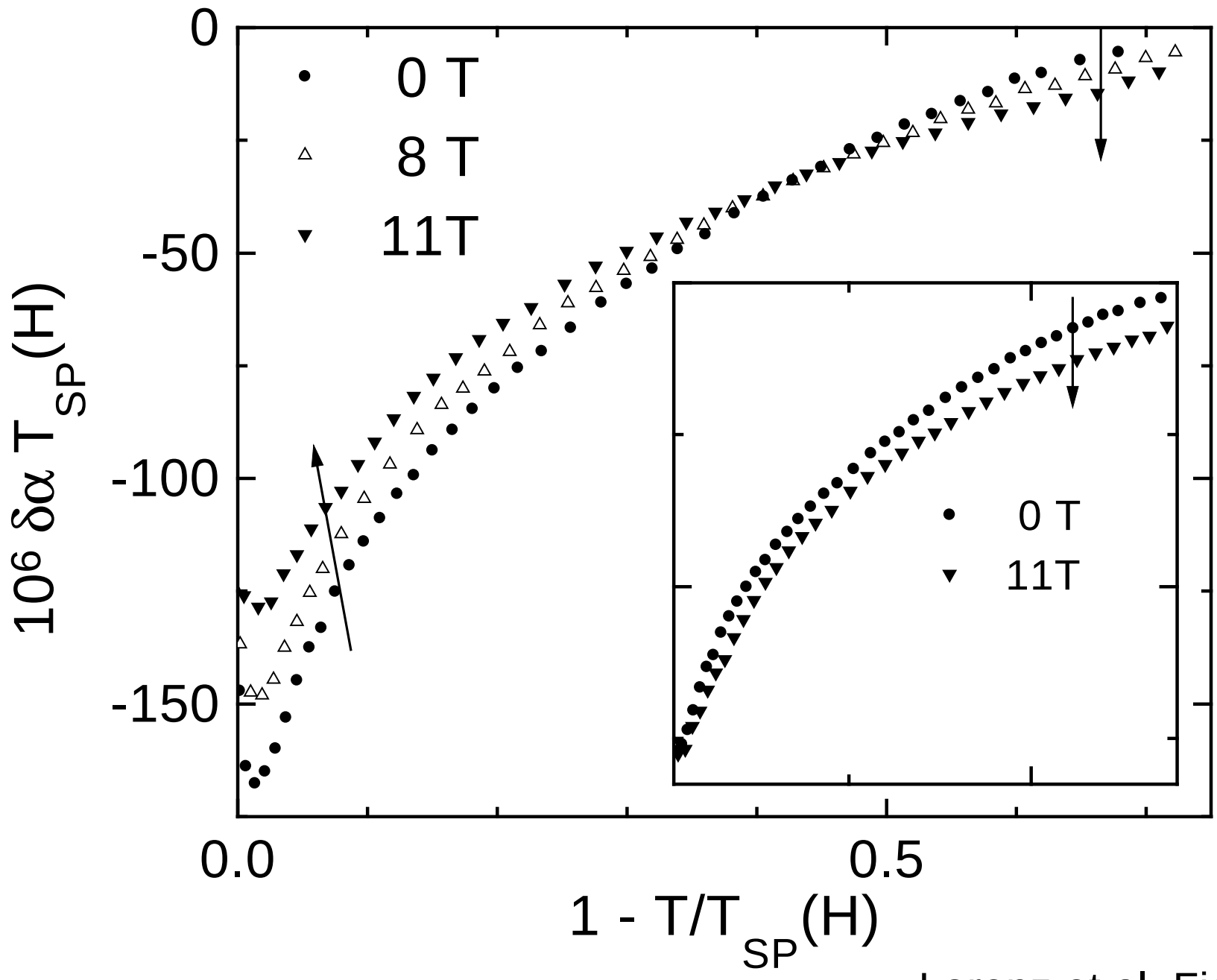


Lorenz et al. Fig. 13

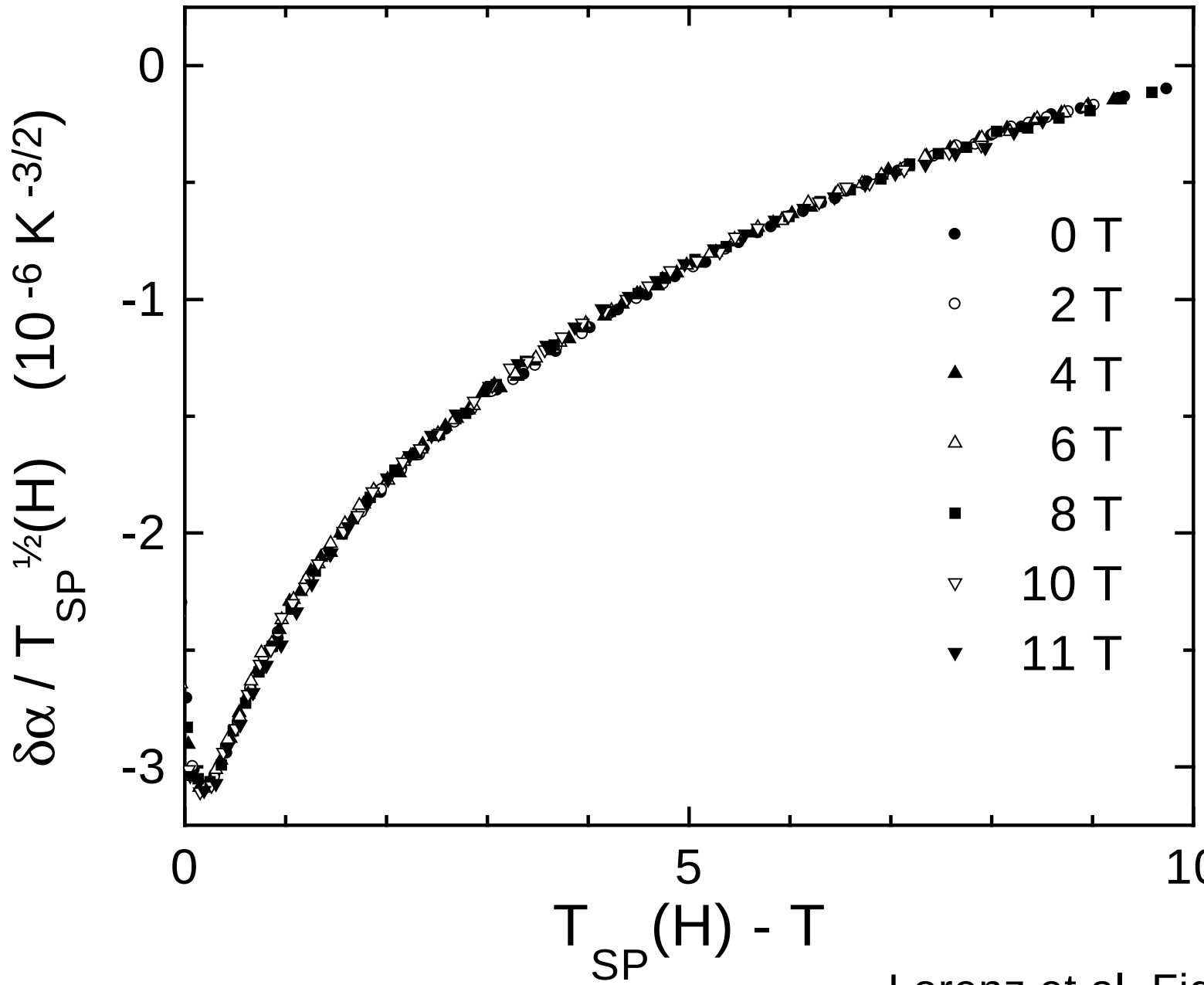


Lorenz et al. Fig. 14

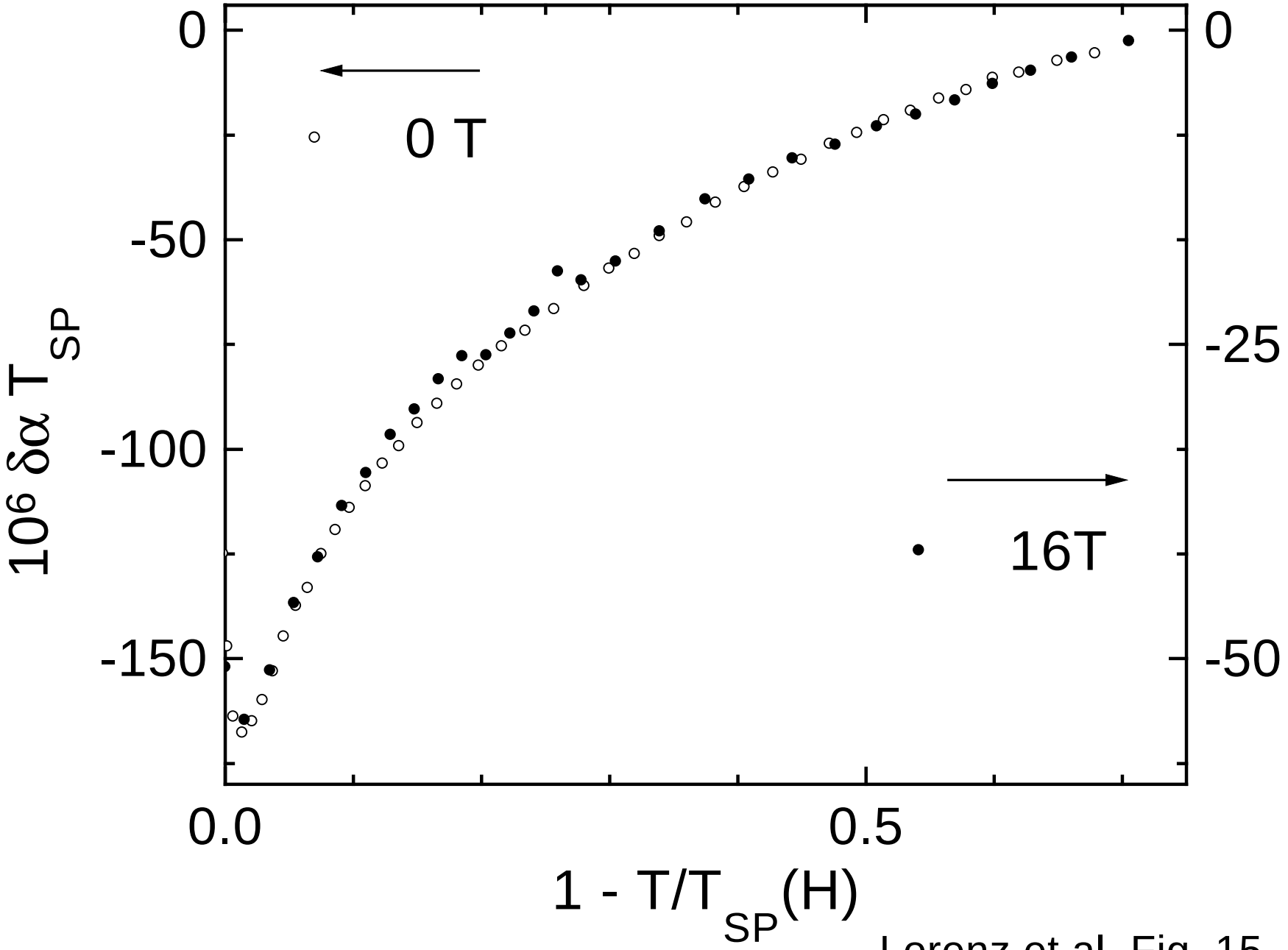


Lorenz et al. Fig. 15